AD

TECHNICAL REPORT ARBRL-TR-02267

PLASMA DYNAMICS OF THE ARC-DRIVEN RAIL GUN

John D. Powell
Jad H. Batteh

September 1980

US ARMY ARMAMENT RESEARCH AND DEVELOPMENT COMMAND
BALLISTIC RESEARCH LABORATORY
ABERDEEN PROVING GROUND, MARYLAND

Destroy this report when it is no longer needed.
Do not return it to the originator.

Secondary distribution of this report by originating or sponsoring activity is prohibited.

Additional copies of this report may be obtained from the National Technical Information Service, U.S. Department of Commerce, Springfield, Virginia 22151.

The findings in this report are not to be construed as an official Department of the Army position, unless so designated by other authorized documents.

The use of trade names or manufacturers' names in this report does not constitute indorsement of any commercial product.

UNCLASSIFIED

SECURITY CLASSIFICATION OF THIS PAGE *(When Data Entered)*

REPORT DOCUMENTATION PAGE		READ INSTRUCTIONS BEFORE COMPLETING FORM
1. REPORT NUMBER TECHNICAL REPORT ARBRL-TR-02267	2. GOVT ACCESSION NO.	3. RECIPIENT'S CATALOG NUMBER
4. TITLE *(and Subtitle)* Plasma Dynamics of the Arc-Driven Rail Gun		5. TYPE OF REPORT & PERIOD COVERED 6. PERFORMING ORG. REPORT NUMBER
7. AUTHOR(s) John D. Powell and Jad H. Batteh*		8. CONTRACT OR GRANT NUMBER(s)
9. PERFORMING ORGANIZATION NAME AND ADDRESS Ballistic Research Laboratory ATTN: DRDAR-BLB Aberdeen Proving Ground, MD 21005		10. PROGRAM ELEMENT, PROJECT, TASK AREA & WORK UNIT NUMBERS RDT&E 1L161102AH43
11. CONTROLLING OFFICE NAME AND ADDRESS US Army Armament Research & Development Command Ballistic Research Laboratory ATTN: DRDAR-BL, APG, MD 21005		12. REPORT DATE SEPTEMBER 1980 13. NUMBER OF PAGES 65
14. MONITORING AGENCY NAME & ADDRESS*(if different from Controlling Office)*		15. SECURITY CLASS. *(of this report)* Unclassified 15a. DECLASSIFICATION/DOWNGRADING SCHEDULE

16. DISTRIBUTION STATEMENT *(of this Report)*

Approved for public release; distribution limited.

17. DISTRIBUTION STATEMENT *(of the abstract entered in Block 20, if different from Report)*

18. SUPPLEMENTARY NOTES

*Present Address: Science Applications, Inc., Atlanta, Georgia

19. KEY WORDS *(Continue on reverse side if necessary and identify by block number)*

Electric gun, rail gun, electromagnetic propulsion, plasma dynamics, fluid mechanics

20. ABSTRACT *(Continue on reverse side if necessary and identify by block number)* (hmn)

A model is analyzed to study the electromagnetic acceleration of particles using a rail gun. Current is conducted between the rails by a plasma arc which accelerates down the rails driving the projectile. The analysis includes determining the electromagnetic fields within the gun and solving the fluid-mechanical equations of the plasma under the assumption that the flow parameters are steady in a frame that accelerates with the arc. Specifically, a set of coupled equations is derived which, when solved, yields the properties of the arc and the

DD FORM 1 JAN 73 1473 EDITION OF 1 NOV 65 IS OBSOLETE UNCLASSIFIED

SECURITY CLASSIFICATION OF THIS PAGE *(When Data Entered)*

acceleration of the projectile. A limiting-case analytic solution to the equations is found, and an iterative technique is employed to solve the equations numerically in the more general case. The results of the calculation are applied to analyze the arc in an experiment recently carried out by Rashleigh and Marshall. In addition, the properties of the arc appropriate for a larger rail gun, such as proposed in a forthcoming experiment by Westinghouse, are investigated and some approximate scaling relations derived. The results of the calculations are compared with those of others and some suggestions for future investigations are given.

TABLE OF CONTENTS

LIST OF FIGURES

LIST OF TABLES

I. INTRODUCTION

Intermittently since World War I, efforts have been directed toward the research and development of a device capable of the electromagnetic acceleration of macroparticles. Such a device has the potential for a number of military applications, probably the most important of which is the so-called electric gun. The major advantage of this sort of gun over the more conventional ones is that, at least in principle, much higher muzzle velocities can be obtained. In addition, the guns should be relatively smokeless and noiseless and their projectiles should experience fairly constant acceleration.

Although the efforts mentioned above have met with varying degrees of success, it has been only since the recent experiments[1-3] at the Australian National University (ANU) that military interest in the problem has been rekindled. These experiments demonstrated conclusively that the 500 MJ homopolar generator, previously developed at ANU, could provide sufficient power to accelerate a mass of about 3g to a velocity of about 6 km/s in a distance of about 3m. The renewed military interest is made evident by the current DARPA/ARRADCOM supported project underway at Westinghouse which has as its goal the acceleration of a 300g mass to a velocity of 3 km/s in a distance of about 4m. If such an objective can be met, the development of an electric gun may become a feasible military goal.

A number of devices exist for producing the electromagnetic acceleration of projectiles, the most notable being the rail gun[1-3] and the mass driver[4,5]. The experiments at ANU and those now underway at Westinghouse were performed using a rail gun and it is with this device that our analysis deals. A schematic of the rail gun is shown in Figure 1. Sides one and two represent the rails which carry current from the source, side three, to and from side four. The projectile is represented by the shaded part of the figure and may, if desired, be a

---

1. S.C. Rashleigh and R.A. Marshall, "Electromagnetic Acceleration of Macroparticles to High Velocities", J. Appl. Phys. 49, 2540 (1978).
2. R.A. Marshall, "The Australian National University Rail Gun Project", Atomic Energy, 16, January 1975.
3. J.P. Barber, "The Acceleration of Macroparticles and a Hypervelocity Electromagnetic Accelerator", Ph.D. Thesis (Australian National University, 1972) (Unpublished).
4. H. Kolm, "Basic Coaxial Mass Driver Reference Design", Third Princeton/AIAA Conference on Space Manufacturing Facilities, Paper No. 77-534, Princeton, NJ, May 1977.
5. K. Fine, "Basic Coaxial Mass Driver Construction and Testing", Third Princeton/AIAA Conference on Space Manufacturing Facilities, Paper No. 77-535, Princeton, NJ, May 1977.

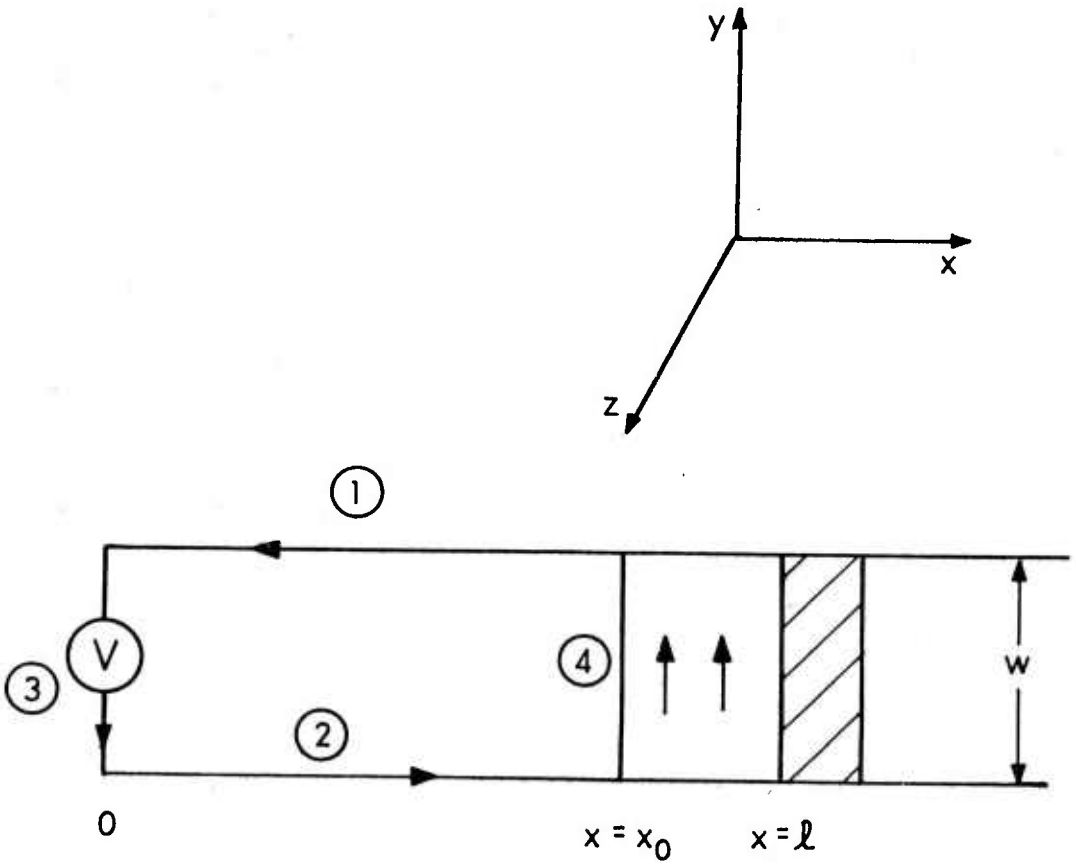

Figure 1. Model for rail gun.

conductor which completes the circuit. There are some advantages, however, to having the projectile an insulator and allowing the current to be conducted by a plasma arc, shown by the region between $x = x_o$ and $x=\ell$. The primary advantages are that better contact with the rails can be maintained by an arc than by a solid armature and that the stress imparted to the projectile is likely to be more uniform. In practice the arc can be created by, for example, an exploding wire. The earliest use of the arc-driven rail gun was apparently in experiments by Brast and Sawle[6] who succeeded in accelerating projectiles of a few mg to velocities of a few km/s. At any rate the current distribution produces a magnetic field in the space bounded by the four sides which interacts with the current through the armature, accelerating it in the x direction.

Some theoretical analysis[3] of the solid-armature rail gun has been carried out and, more recently, McNab[7] has undertaken the more difficult task of obtaining some estimates of the properties of the arc in the arc-driven gun. Although these calculations provide considerable insight into the problem as well as good qualitative results, they are based upon a number of assumptions which are unlikely to be strictly valid for the problem at hand. It is assumed in McNab's analysis, for example, that the pressure, density, and temperature within the arc are uniform although it is unlikely that all three flow variables will be constant in an arc that does not move at constant velocity. In addition, it is assumed that atoms which constitute the arc are, at most, singly ionized. However, the results of the calculation indicated that the temperature of the arc was about 57,000°K, and one can show[8] that at this high temperature most of the atoms should be ionized to a higher degree.

The inadequacy of these assumptions in no way detracts from McNab's work since, as pointed out, the results do appear to be qualitatively reliable and the calculations are rather straightforward to carry out. In the present analysis, however, we wish to extend the work. In particular, we will solve the fluid-dynamical equations in the accelerating arc and, thereby, account for the position dependence of the flow variables where necessary. In addition, it will be assumed that the plasma may consist of doubly ionized as well as singly ionized atoms. The results will be applied to the Rashleigh-Marshall (RM) experiment[1] and compared briefly to the results obtained by McNab. The question of how the arc should be scaled for a rail gun of the size proposed in the Westinghouse experiment will then be examined, and the properties of the arc under those conditions will be investigated.

6. D.E. Brast and D.R. Sawle, "Study of a Rail-Type MHD Hypervelocity Projectile Accelerator", Proc. Seventh Hypervelocity Impact Symposium, 1964, Vol. 1, p. 187 (unpublished).
7. I. McNab, "Electromagnetic Acceleration by a High Pressure Plasma", J. Appl. Phys. 51, 2549 (1980).
8. Authors' unpublished calculations.

The report is organized as follows. In Sec. II, the model and assumptions are discussed briefly. In Sec. III, the formal analysis of the problem is presented, including the derivation of a set of coupled equations which must be solved to determine the properties of the arc and the motion of the projectile. In Sec. IV, a limiting-case analytic solution to the equations is found and their numerical solution for the more general case is discussed. The results are then applied to both the RM experiment and to the proposed Westinghouse experiment. Finally, in Sec. V, some additional discussion of the results, the assumptions, and possible future investigations is given.

II. MODEL AND ASSUMPTIONS

The model whose properties we wish to consider consists of an arc-driven rail gun such as shown in Figure 1. The rails are assumed to be perfectly conducting, infinitely thin sheets which are infinitely extended in the z direction, as is the arc. The gun itself is therefore two dimensional, although the fluid-mechanical properties of the arc are assumed to vary only in the direction of propagation. Certainly the major variation does occur in that direction because of the purely mechanical effect of accelerating the arc. However, in a real system some variations occur in directions normal to the propagation direction, and these are not accounted for in the model. The finite conductivity σ of the arc is accounted for, and the assumption that the rails are perfect conductors is justified on the basis that, in reality, the conductivity of the rails is several orders of magnitude higher than that of the arc. The potential difference V which is applied along side three of the model is assumed to vary with time so as to produce a constant current per unit height j on the surface of the rails. In practice, such a condition can be approximated by using as a source an inductive store of sufficiently high inductance.

We will be interested in solving the equations which govern the properties of the arc and the acceleration of the projectile in the steady-state approximation. By steady state we mean that the acceleration of the projectile and all parts of the arc is the same at any given time, and that the fluid-mechanical properties of the arc are independent of time in a frame which accelerates with the arc. It is, of course, also assumed that the mass of the arc is constant in time so that any vaporization of the rails is neglected during the time of acceleration. A number of specific criteria which must be satisfied to justify the assumption of steady state are discussed in the ensuing pages. In particular, this assumption, as well as the others, is discussed in some detail in Sec. V.

III. ANALYSIS

A. Electrodynamics.

The first problem which must be solved is to determine the electromagnetic fields associated with the arc gun in Figure 1. From the symmetry of the problem and from the results[9] of similar calculations, we assume solutions to Maxwell's equations of the form

$$\vec{E} = E(x)\ \hat{a}_y$$
$$\vec{B} = B(x)\ \hat{a}_z \tag{3.1}$$

where $\vec{E}$ and $\vec{B}$ are the electric and magnetic induction fields, respectively. The appropriate Maxwell equations then become*

$$\frac{\partial E}{\partial x} = \frac{-\partial B}{\partial t} \tag{3.2a}$$

and

$$\frac{\partial B}{\partial x} = -\mu J \tag{3.2b}$$

where μ is the magnetic permeability and J the current density to be determined within the arc. In writing Eq. (3.2b) we have neglected the displacement current which is negligible for nonrelativistic velocities of the arc and projectile.

Equation (3.2b) implies that $\vec{B}$ is constant except within the arc, and since it must vanish at infinity, it vanishes everywhere to the right of $x = \ell$, to the left of $x = 0$, and above and below the perfectly conducting rails. Within the arc Eq. (3.2b) implies

$$B = -\mu \int_{x_o}^{x} J\, dx + c \tag{3.3}$$

where c is an integration constant which can be determined from the continuity of B and from the boundary condition

$$B(\ell) = -\mu \int_{x_o}^{\ell} J(x)dx + c = 0. \tag{3.4}$$

We have, therefore,

---

9. R.M. Fano, L.J. Chu, and R.B. Adler, Electromagnetic Fields, Energy, and Forces (Wiley, New York, 1960), Chap. 9.

* Unless otherwise noted, MKS units are used throughout this report.

$$B = \mu \int_{x}^{\ell} J \, dx, \tag{3.5}$$

for $x_o \leq x \leq \ell$.

In the space between x=0 and $x=x_o$, B is again constant and to satisfy the boundary condition at $x=x_o$ we must have

$$B = \mu \int_{x_o}^{\ell} J \, dx \, . \tag{3.6}$$

However, the integral on the right of Eq. (3.6) must just be equal to j, the current per unit height on the rails, if current is to be conserved in the steady state. Consequently, we have

$$B = \mu j, \tag{3.7}$$

for $0 < x \leq x_o$.

The electric field $\vec{E}$ can be determined most simply by making the change of variable

$$x' = x - x_o(t) \tag{3.8}$$

in Eq. (3.2a). For steady-state conditions we find

$$\frac{\partial E}{\partial x'} = v \frac{\partial B}{\partial x'} \tag{3.9}$$

where

$$v = \frac{dx_o}{dt} \tag{3.10}$$

is the common velocity of the arc and projectile. Integrating Eq. (3.9), we find

$$E = vB + F(t) \tag{3.11}$$

where F(t) is an arbitrary function to be determined.

The function F(t) can be evaluated by noting that the current density in the arc must obey the constitutive relation

$$J = \sigma(E - vB). \tag{3.12}$$

Thus, F(t) is given simply by

$$F(t) = J/\sigma \ . \tag{3.13}$$

Furthermore, for the assumed steady conditions, the quantity J/σ is independent of time so

$$E = E_o + vB, \tag{3.14}$$

where the constant

$$E_o = J/\sigma \tag{3.15}$$

represents the electric field required to drive the current through the arc. If we make use of the current-conservation relation mentioned earlier, namely,

$$\int_{x_o}^{\ell} J(x)dx = j, \tag{3.16}$$

E_o can be written in terms of known quantities as

$$E_o = \frac{j}{\int_{x_o}^{\ell} \sigma(x)dx} \ . \tag{3.17}$$

In the remaining discussion we will need the values of $\vec{E}$ and $\vec{B}$ only to the right of $x=x_o$ and between the perfectly conducting rails. Writing these in terms of the dimensionless distance ξ defined by

$$\xi = (x - x_o)/\ell_a \ , \tag{3.18}$$

we have

$$\begin{aligned} \vec{B} &= \mu \ell_a E_o \int_{\xi}^{1} \sigma(\xi)\, d\xi\, \hat{a}_z \qquad && 0 \leqslant \xi \leqslant 1 \\ \vec{B} &= 0. && \xi > 1 \ . \end{aligned} \tag{3.19}$$

In these equations ℓ_a is the length of the arc measured along the x axis, viz.,

$$\ell_a = \ell - x_o. \tag{3.20}$$

Similarly,

$$\vec{E} = [\, E_o + vB(\xi)] \, \hat{a}_y \tag{3.21}$$

for $\xi > 0$ where E_o is given by Eq. (3.17).

The solutions obtained in this section can be seen to satisfy all boundary conditions appropriate to the problem and the assumption made in Eq. (3.1) is therefore justified. A more arduous derivation[10], employing the vector potential and avoiding the assumption, produces the same result.

B. Fluid Mechanics.

Having obtained the values of the electric and magnetic fields, we now wish to derive a set of equations appropriate for determining the fluid-mechanical properties of the arc. The equations which express conservation of mass, momentum, and energy for the arc as a whole can be written[11]

$$\begin{aligned} &\frac{\partial \rho}{\partial t} + \frac{\partial}{\partial x}(\rho v) = 0 \\ &\rho \frac{\partial v}{\partial t} + \rho v \frac{\partial v}{\partial x} + \frac{\partial P_{xx}}{\partial x} = f \\ &\rho \frac{\partial e}{\partial t} + \rho v \frac{\partial e}{\partial x} + \frac{\partial q}{\partial x} + P_{xx} \frac{\partial v}{\partial x} = J^2/\sigma \end{aligned} \tag{3.22}$$

where ρ is the mass density in the arc, v the mean flow velocity, e the specific internal energy, q the heat flux, f the force per unit volume acting on the plasma, and P_{xx} the appropriate element of the pressure tensor for one-dimensional considerations. Equations (3.22) are identical to those generally encountered in fluid mechanics except for the force f which is electromagnetic in origin and except for the term J^2/σ which represents the Joule heating of the plasma. In compliance with the assumptions previously discussed, the flow variables have been assumed to vary only in the direction of propagation of the arc.

It is clear that the three equations in Eqs. (3.22) cannot uniquely specify the variables P, ρ, v, and e and one needs, in addition, an equation of state. We assume, therefore, that the plasma obeys an ideal-gas law, namely,

10. Authors' unpublished calculations.
11. A.B. Cambel, Plasma Physics and Magnetofluidmechanics (McGraw-Hill, New York, 1963), Chap. 8.

$$P = (1 + \alpha)\, \rho\, \frac{k_B T}{m_o} \tag{3.23}$$

where k_B is Boltzmann's constant, T the temperature, m_o the atomic mass of the ion or neutral, and α the ratio of electrons to heavy particles in the plasma. The method for determining α will be discussed in the following section. All flow variables are assumed to vary only slowly with position so that the gas is in a state of local thermal equilibrium.

Further analysis of Eqs. (3.22) is most easily accomplished in a frame moving with the velocity v of the plasma arc. We therefore make the change of variable defined in Eq. (3.18). Noting that in the moving frame v is independent of ξ and that ρ, e, and P are independent of time, we find that the first of Eqs. (3.22) is satisfied identically, while the remaining two become

$$\rho a + \frac{1}{\ell_a} \frac{\partial P}{\partial \xi} = f \tag{3.24}$$

and

$$\frac{\partial q}{\partial \xi} = \ell_a\, J^2/\sigma \ . \tag{3.25}$$

In Eq. (3.24) a represents the common acceleration of the arc and projectile and P_{xx} has been replaced by the pressure, P, since no velocity gradients are assumed to exist.

The force per unit volume f acting on the plasma arises from the interaction of the magnetic induction field within the arc and the current through it. The force acts in the positive x direction and its magnitude is given by [12]

$$f = JB \ . \tag{3.26}$$

Consequently, Eq. (3.24) can be written in the form

$$P(\xi) = \ell_a \int_o^{\xi} \left[J(\xi)\, B(\xi) - \rho(\xi) a \right] d\xi + c \tag{3.27}$$

where c is an integration constant which can be determined from the condition that the pressure at the back of the projectile must be sufficient to provide it with an acceleration a. Specifically, if we let

12. J.D. Jackson, Classical Electrodynamics (Wiley, New York, 1962), Chap. 5.

ρ_{ℓ_p} represent the density of the projectile multiplied by its length along the x axis, we must have

$$P(\xi=1) = \ell_a \int_0^1 (JB-\rho a)d\xi + c = \rho_{\ell_p} a \ . \tag{3.28}$$

It is clear, however, that the term JB, integrated over the entire volume of the arc, yields the <u>total</u> force acting on the arc and projectile so

$$(\rho_{\ell_p} + \rho_{\ell_a})a = \ell_a \int_0^1 J(\xi)\ B(\xi)\ d\xi \tag{3.29}$$

where ρ_{ℓ_a} represents the average arc density multiplied by its length along the x axis. In the appendix it is proved that the acceleration a is independent of how the current is distributed in the arc; in fact, the simple expression

$$a = \frac{\mu j^2}{2\left(\rho_{\ell_a}+\rho_{\ell_p}\right)} \tag{3.30}$$

is obtained. At any rate, Eqs. (3.28) and (3.29) imply c=0, so we have at last

$$P(\xi) = \ell_a \int_0^{\xi} [J(\xi)\ B(\xi) - \rho(\xi)a]\ d\xi. \tag{3.31}$$

The second term on the right-hand side of Eq. (3.31) is clearly negligible with respect to the first provided $\rho_{\ell_a} << \rho_{\ell_p}$ as it is under most conditions.

From Eq. (3.23) the mass density of the arc is given by

$$\rho = \frac{m_o P}{k_B T(1+\alpha)} \tag{3.32}$$

and the length of the arc can be determined from the condition

$$\ell_a \int_0^1 \rho(\xi)d\xi = \rho_{\ell_a} \ . \tag{3.33}$$

Solving for ℓ_a, we obtain

$$\ell_a = \rho_{\ell_a} \Big/ \int_0^1 \rho(\xi)\,d\xi \quad . \tag{3.34}$$

The parameter ρ_{ℓ_a} is, of course, independent of ℓ_a.

Provided the temperature of the arc is sufficiently high, heat is transferred within the arc and to its surroundings primarily by radiation and conduction can be neglected. Therefore, q in Eq. (3.25) can be taken to represent the heat flux due to radiation, and we have upon integration

$$q = \ell_a \int_0^{\xi} \frac{J^2}{\sigma}\,d\xi + c \quad . \tag{3.35}$$

The constant of integration c can be determined from the fact that at the interface between the arc and the (assumed) vacuum behind it (ξ=0), the flux must approximately reduce to[13]

$$q(0) = -\,2\sigma_s T_o^{\,4}, \tag{3.36}$$

where T_o is the temperature of the arc at $\xi = 0$ and σ_s is Stefan's constant, namely, 5.67×10^{-8} $\frac{J}{m^2 deg^4 s}$. Consequently, we have

$$q = \ell_a \int_0^{\xi} J^2/\sigma\,d\xi - 2\sigma_s T_o^{\,4} \quad , \tag{3.37}$$

where the unknown temperature T_o must be determined.

If the radiative mean free path within the arc is small compared to the arc length, as we shall find to be the case, the flux q can be approximated by the "radiative heat conduction" equation,[13]

13. Y.B. Zel'dovich and Y.P. Raizer, Physics of Shock Waves and High-Temperature Hydrodynamic Phenomena (Academic, New York, 1966), Vol. I, Chap. 2.

$$q = \frac{-16\,\sigma_s\,\lambda\,T^3}{3\,\ell_a}\,\frac{dT}{d\xi}\,, \tag{3.38}$$

where λ represents the mean free path for radiation averaged over the entire frequency spectrum. Obviously to solve the equation an additional boundary condition must be specified. To obtain the condition we note that during the entire time of acceleration energy is transferred to the projectile surface, continuously heating its interior. As the projectile temperature rises, the transfer of energy from arc to projectile becomes less efficient, and this change in the transfer rate with time will clearly produce a time-dependent effect on the temperature in the arc. Thus, in a strict sense, the temperature profile of the arc is not completely steady. It is clear, however, that the projectile temperature at any time is substantially less than that of the arc and, consequently, little error should be made in assuming that the arc at the projectile surface is maintained at some constant temperature. Furthermore, since the radiative mean free path is small compared to the arc length, the properties of the arc, except very near the boundary, should be independent of this temperature. For these reasons it is convenient to assume that the projectile absorbs all the radiation which is incident upon it, just as does the vacuum behind the arc, and therefore the flux at $\xi=1$ reduces to

$$q(1) = 2\,\sigma_s T_1^{\,4}\,, \tag{3.39}$$

where T_1 is the arc temperature at the projectile surface. This condition supplies, then, the additional boundary condition. Further discussion of this assumption is given in Sec. V.

We have, upon integrating Eq. (3.38),

$$T^4 = \frac{3\ell_a}{4\sigma_s}\int_{\xi}^{1}\frac{q}{\lambda}\,d\xi + T_1^{\,4}\,. \tag{3.40}$$

From Eqs. (3.37), (3.39), and (3.40), we obtain for the unknown temperatures T_o and T_1 the relationships

$$T_o^4 = \frac{3\ell_a}{4\sigma_s}\int_{o}^{1}\frac{q}{\lambda}\,d\xi + T_1^{\,4} \tag{3.41}$$

and

$$T_1^{\,4} = \frac{\ell_a}{2\sigma_s}\int_{o}^{1}\frac{J^2}{\sigma}\,d\xi - T_o^{\,4}\,. \tag{3.42}$$

Solving for T_o and T_1 and substituting in Eqs. (3.37) and (3.40) we find

$$q = \ell_a \int_o^\xi \frac{J^2}{\sigma}\, d\xi - \frac{\ell_a}{2} \int_o^1 \frac{J^2}{\sigma}\, d\xi - \frac{3\ell_a}{4} \int_o^1 \frac{q}{\lambda}\, d\xi \qquad (3.43)$$

and

$$T = \left\{ \frac{3\ell_a}{4\sigma_s} \int_\xi^1 \frac{q}{\lambda}\, d\xi + \frac{\ell_a}{4\sigma_s} \int_o^1 \frac{J^2}{\sigma}\, d\xi - \frac{3\ell_a}{8\sigma_s} \int_o^1 \frac{q}{\lambda}\, d\xi \right\}^{1/4} . \qquad (3.44)$$

Equations (3.43) and (3.44) provide two coupled equations for the heat flux q and temperature T. Formally the equations can be solved by the transformation

$$q = A + F(\xi) . \qquad (3.45)$$

After substitution into Eq. (3.43) we find

$$F(\xi) = \ell_a \int_o^\xi \frac{J^2}{\sigma}\, d\xi \qquad (3.46)$$

and

$$A = - \left[\frac{E_o j}{2} + \frac{3\ell_a}{4} \int_o^1 \frac{F(\xi)}{\lambda}\, d\xi \right] \Big/ \left[1 + \frac{3\ell_a}{4} \left\langle \frac{1}{\lambda} \right\rangle \right] \qquad (3.47)$$

where $\langle 1/\lambda \rangle$ is the inverse of the mean free path averaged over the length of the arc, i.e.,

$$\left\langle \frac{1}{\lambda} \right\rangle = \int_o^1 \frac{1}{\lambda}\, d\xi . \qquad (3.48)$$

Equation (3.44) can now be written

$$T = \left\{ \frac{3\ell_a}{4\sigma_s} \int_\xi^1 \frac{q}{\lambda}\, d\xi + \frac{E_o j}{4\sigma_s} - \frac{3\ell_a A}{8\sigma_s} \left\langle \frac{1}{\lambda} \right\rangle - \frac{3\ell_a}{8\sigma_s} \int_o^1 \frac{F(\xi)}{\lambda}\, d\xi \right\}^{1/4} . \qquad (3.49)$$

C. Degree of Ionization.

The parameter α, occurring in Eq. (3.23), must be obtained before a solution to the fluid-mechanical equations considered in the last section can be found. In practice, this parameter results from the solution of a hierarchy of equations generally referred to simply as the Saha equation. In this section we outline the method by which the solution is obtained. For greater detail the reader is referred to the literature[14].

We recall that the parameter α represents the ratio of the number of electrons to the number of heavy particles, N_H. We let x_j be the ratio of the number of atoms ionized j times (referred to as "j^{th} ions") to N_H. It is then evident that α is given by

$$\alpha = \sum_j j\, x_j \tag{3.50}$$

and the electron number density in the arc by

$$n_e = \frac{\rho\alpha}{m_o} \quad . \tag{3.51}$$

The x_j's are obviously normalized such that

$$\sum_j x_j = 1. \tag{3.52}$$

In Eqs. (3.50) and (3.52), the sums over j run over all values for which appreciable ionization occurs.

It has been shown that the x_j's satisfy the following system of equations, usually called the Saha equation:

$$\frac{x_{j+1}\,\alpha}{x_j\,(1+\alpha)} = \frac{2}{P}\,\frac{Z_{j+1}}{Z_j}\left(\frac{m_e}{2\pi\hbar^2}\right)^{3/2}(k_B T)^{5/2}\, e^{-I_{j+1}\,/\,k_B T} = K_{j+1}(T,P). \tag{3.53}$$

In Eqs. (3.53) $\hbar$ is Planck's constant divided by 2π, m_e the electron mass, I_j the ionization energy needed to ionize the atom j times, and the Z_j's are electronic partition functions for the j^{th} ion. Specifically, Z_j is given by

14. See Ref. 13, Chapter 3.

$$Z_j(\xi) = \sum_i g_{ji}\, e^{-U_{ji}/k_B T(\xi)} \tag{3.54}$$

where U_{ji} is the energy of the i^{th} electronic state of the j^{th} ion and where g_{ji} is the appropriate degeneracy factor for this level. The partition functions depend upon position in the arc since the temperature is a function of position in the problem under consideration. Similarly, the x_j's are also position dependent.

Equations (3.53) are deceptively simple looking. In practice the equation for any x_j always depends on x_{j+1} and, thus, the system of equations must be terminated at some point. If, for example, we assume that only single ionization occurs, then,

$$\alpha = x_1, \tag{3.55}$$

and only the term corresponding to j=0 is retained in Eqs. (3.53). The single resulting equation becomes

$$\frac{x_1^2}{1-x_1^2} = K_1(T,P) \tag{3.56}$$

if we use Eqs. (3.50) and (3.52). If desired, the equation can be solved for x_1 (or α), and substituted into the fluid-dynamic equations of the previous section.

For the problem under study here, however, it is usually insufficient to assume only single ionization. In the event that double ionization is also allowed,

$$\alpha = x_1 + 2x_2 \tag{3.57}$$

and Eqs. (3.53) become

$$\begin{aligned} \frac{x_1(x_1+2x_2)}{(1-x_1-x_2)(1+x_1+2x_2)} &= K_1(T,P) \\ \frac{x_2(x_1+2x_2)}{x_1(1+x_1+2x_2)} &= K_2(T,P). \end{aligned} \tag{3.58}$$

Again we have used Eqs. (3.50) and (3.52). These equations are most easily solved by iteration. After considerable algebra, they can be rewritten in the form

$$x_1 = \frac{K_1 x_2}{2K_2} \left\{ \left[1 + \frac{4K_2(1-x_2)}{K_1 x_2} \right]^{1/2} - 1 \right\} \tag{3.59}$$

$$x_2 = \frac{K_2}{K_1 \left\{ \left[1 + \frac{4K_2(1-x_2)}{K_1 x_2} \right]^{1/2} - 1 \right\}} \cdot \frac{(2+3K_1)x_2}{1+K_1} \left\{ \left[\frac{4K_1(1+K_1)(1+x_2-2x_2^2)}{x_2^2(2+3K_1)^2} + 1 \right]^{1/2} - 1 \right\}. \tag{3.60}$$

A value for x_2 is then assumed, substituted into the right-hand side of Eq. (3.60) and a new value of x_2 calculated. The process is then repeated until successive values agree to within any desired accuracy. The value for x_1 then follows directly from Eq. (3.59).

To illustrate the results we have plotted in Figure 2 values of x_1 and x_2 as a function of log T for a pressure of 10^7 N/m^2. The plasma was assumed to be a gas of partially ionized copper atoms. The partition functions in Eq. (3.54) were calculated using values[15] for the g_{ji} and U_{ji} shown in Table I. Calculations were undertaken retaining first ten, and then fifteen, terms in the partition functions and no discernible differences were found in the results. The initial value of x_2 was chosen to be 0.01 and successive values were found to agree to within one part in 10^5 after, at most, a few tens of iterations. As can be seen from the graph no appreciable ionization exists below log T $\approx$ 9 (T=8,100°K). Second ionization is negligible below log T $\approx$ 10 (T = 22,000°K) and then rises fairly rapidly. Once x_2 has become large (above, say, log T $\approx$ 10.5 or T = 36,000°K), triple ionization is probably also important, but is not accounted for in the analysis above.

D. Summary of Governing Equations.

In the analysis of the preceding sections we have derived a system of coupled equations sufficient to determine the electromagnetic fields, the acceleration of the projectile, and the fluid-mechanical properties

15. Data taken from C.E. Moore, "Atomic Energy Levels", National Bureau of Standards Circ. No. 467, V. II, Washington, DC, 1952.

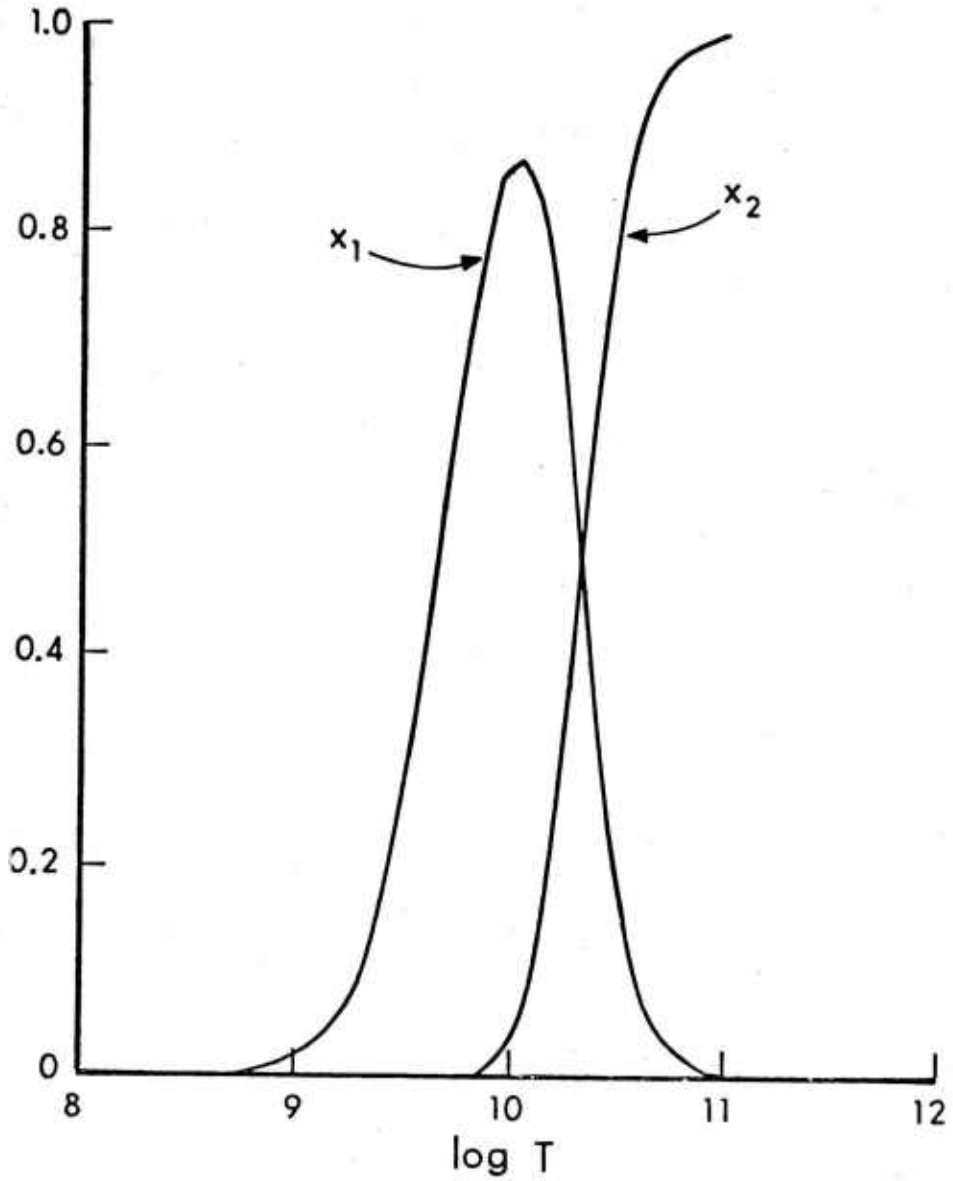

Figure 2. Ionization factors as a function of temperature.

Table I. Atomic Energy Levels and Degeneracy Factors for Copper and Its Ions. Energies are expressed in °K (from Ref. 15).

	j = 0 I_1 = 89638		j = 1 I_2 = 235420		j = 2 I_3 = 427354	
i	g_{0i}	U_{0i}	g_{1i}	U_{1i}	g_{2i}	U_{2i}
0	2	0	1	0	6	0
1	6	16114	7	31543	4	2980
2	4	19052	5	32863	10	87463
3	2	43923	3	34520	8	89276
4	4	44280	5	37779	6	90827
5	6	56125	5	95538	4	91895
6	4	57701	3	96793	8	96398
7	2	58894	1	99036	6	99198
8	9	58844	9	98864	6	112150
9	8	59196	7	98457	4	113316
10	6	59785	5	100500	2	115682
11	4	60849	9	100265	4	115513
12	2	62049	7	102892	6	115867
13	8	62591	5	104607	4	112908
14	6	63874	7	101900	2	123895

of the arc. For easy reference the most pertinent equations are listed below [see Eqs. (3.15), (3.17), (3.19), (3.30), (3.31), (3.32), (3.34), (3.45), (3.46), (3.47), (3.49), (3.50), (3.51), (3.59), and (3.60)]:

$$J = \sigma E_o \tag{3.61}$$

$$E_o = \frac{j}{\ell_a \int_o^1 \sigma(\xi) d\xi} \tag{3.62}$$

$$B = \mu \ell_a \int_\xi^1 J(\xi) d\xi \tag{3.63}$$

$$a = \frac{\mu j^2}{2\left(\rho_{\ell_a} + \rho_{\ell_p}\right)} \tag{3.64}$$

$$P = \ell_a \int_o^\xi \left[J(\xi)B(\xi) - \rho(\xi)\, a\right] d\xi \tag{3.65}$$

$$\rho = \frac{m_o P}{k_B T(1+x_1+2x_2)} \tag{3.66}$$

$$\ell_a = \frac{\rho_{\ell_a}}{\int_o^1 \rho(\xi) d\xi} \tag{3.67}$$

$$q = A + F(\xi) \tag{3.68}$$

$$T = \left\{ \frac{3\ell_a}{4\sigma_s} \int_\xi^1 \frac{q}{\lambda} d\xi + \frac{E_o j}{4\sigma_s} - \frac{3\ell_a A}{8\sigma_s} \left\langle \frac{1}{\lambda} \right\rangle - \frac{3\ell_a}{8\sigma_s} \int_o^1 \frac{F(\xi)}{\lambda} d\xi \right\}^{1/4} \tag{3.69}$$

$$n_e = \frac{\rho(x_1+2x_2)}{m_o} \tag{3.70}$$

$$x_1 = \frac{K_1 x_2}{2K_2} \left\{ \left[1 + \frac{4K_2(1-x_2)}{K_1 x_2} \right]^{1/2} - 1 \right\} \tag{3.71}$$

$$x_2 = \frac{K_2}{K_1 \left\{ \left[1 + \frac{4K_2(1-x_2)}{K_1 x_2} \right]^{1/2} - 1 \right\}} \cdot \frac{(2+3K_1)x_2}{1+K_1} \left\{ \left[\frac{4K_1(1+K_1)(1+x_2-2x_2^2)}{x_2^2(2+3K_1)^2} + 1 \right]^{1/2} - 1 \right\} . \tag{3.72}$$

In writing Eqs. (3.61) - (3.72) we have assumed that the plasma is at most doubly ionized. If we are provided with appropriate expressions for the conductivity σ and the mean free path λ, the equations are sufficient to determine the twelve unknowns: J, B, P, ρ, T, q, n_e, x_1, x_2, E_o, a, and ℓ_a. The first nine of the unknowns are position dependent, whereas the last three are constant.

IV. SOLUTION OF EQUATIONS

A. Limiting-Case Analytic Solution.

In this section we will be concerned primarily with the numerical solution of the equations summarized in Sec. IIID and their application to the experimental data. Before turning to the numerical results, however, we will present a limiting-case analytic solution which is valid whenever (1) the mass of the arc is negligibly small with respect to the mass of the projectile, (2) the conductivity of the arc is constant, and (3) the radiative mean free path is inversely proportional to the pressure. The analytic solution serves as a useful check for the computer program used to evaluate the numerical results and provides some physical insight into the behavior of the equations as well. In addition, the above assumptions are not totally unreasonable for the problems which will be considered as will be seen when the more general numerical results are presented.

For constant conductivity, Eqs. (3.61) and (3.62) imply

$$J = \frac{j}{\ell_a} \tag{4.1}$$

so the current is uniformly distributed throughout the arc as expected. Equation (3.63) then becomes

$$B = \mu j(1-\xi) \tag{4.2}$$

and the magnetic induction field varies linearly from the value μj at the trailing edge of the arc to zero at the leading edge. Similarly, if we neglect the second term on the right-hand side in Eq. (3.65) in compliance with the first assumption above we have

$$P = \mu j^2(\xi-\xi^2/2). \tag{4.3}$$

Under assumption (3) above, we have from Eq. (4.3)

$$\lambda = \frac{\lambda_o}{\xi-\xi^2/2} \tag{4.4}$$

where λ_o is a constant independent of position within the arc*. Equations (3.46) and (3.47) can now be evaluated and yield for the limiting-case solution

$$F(\xi) = \frac{j^2\xi}{\ell_a\sigma_o} \tag{4.5}$$

and

$$A = \frac{-5j^2}{8\sigma_o\ell_a}\left[1 + \frac{16\lambda_o}{5\ell_a}\right]\Bigg/\left[1 + \frac{4\lambda_o}{\ell_a}\right] \tag{4.6}$$

where σ_o denotes the constant conductivity of the arc. In obtaining Eq. (4.6) we have noted that $< 1/\lambda >$ is simply $1/3\lambda_o$ when Eq. (4.4) is applicable. Provided the mean free path is small compared to the arc length, Eq. (4.6) can be expanded in powers of λ_o/ℓ_a to obtain

$$A \approx \frac{-5j^2}{8\sigma_o\ell_a}\left[1 - \frac{4\lambda_o}{5\ell_a}\right] . \tag{4.7}$$

*It may be seen that $\lambda \to \infty$ as $\xi \to 0$, contradicting our statement that $\lambda << \ell_a$ within the arc. As we shall see, however, reasonable values of λ_o are of the order of 10^{-4}m while ℓ_a is of the order 0.1m, so the condition is violated only very near the boundary. In fact, we found $\lambda<\ell_a$ over 98% of the arc in our numerical calculations. The small error incurred in the calculation resulting from the lack of validity, say, of radiative heat conduction in this small region is deemed negligible.

The expressions for $F(\xi)$ and A can now be used to determine the heat flux q and temperature T within the arc. The flux follows directly from Eq. (3.68) and yields

$$q = \frac{j^2}{\ell_a \sigma_o} \left(\xi - 5/8\right) + O(\lambda_o/\ell_a) \tag{4.8}$$

where $O(\lambda_o/\ell_a)$ denotes higher-order terms in the parameter λ_o/ℓ_a. Thus, the flux changes sign approximately five-eighths of the distance between the trailing edge of the arc, where it is negative, and the leading edge, where it is positive. The asymmetric nature of the flux results from the fact that the mean free path is a function of position.

Substituting Eqs. (4.4) and (4.5) into Eq. (3.69) and evaluating the results we find

$$T^4 = \frac{j^2}{64\sigma_s \sigma_o \lambda_o} \left[20 \frac{\lambda_o}{\ell_a} + 15(1-4\lambda_o/5\ell_a)\xi^2 - 21(1-4\lambda_o/21\ell_a)\xi^3 + 6\,\xi^4 \right] + O(\lambda_o^2/\ell_a^2) \,. \tag{4.9}$$

In the interior part of the arc where $0 < \xi < 1$, the terms of order λ_o/ℓ_a can be neglected in Eq. (4.9) and we have

$$T = \left[\frac{3j^2\xi^2(5-2\xi)(1-\xi)}{64\lambda_o \sigma_s \sigma_o} \right]^{1/4} . \tag{4.10}$$

Here the temperature is independent of ℓ_a as should be expected for $\lambda_o/\ell_a << 1$. Very near the projectile, however, as $\xi \to 1$, the lowest-order terms in Eq. (4.9) vanish and terms proportional to λ_o/ℓ_a must be retained. We obtain then

$$T = \left[\frac{3j^2}{16\ell_a \sigma_s \sigma_o} \right]^{1/4} . \tag{4.11}$$

Similarly, as $\xi \to 0$, or at the trailing edge of the arc, we find

$$T = \left[\frac{5j^2}{16\ell_a \sigma_s \sigma_o} \right]^{\frac{1}{4}} . \qquad (4.12)$$

Very near the boundaries of the arc, then, the temperature does depend on ℓ_a and is lower than that at the center of the arc by a factor of the order of $(\lambda_o/\ell_a)^{\frac{1}{4}}$. The physical meaning of these results will be discussed in some greater detail when the numerical solutions are presented.

The solutions presented above should offer some insight into the physical meaning of the results when we attempt to interpret the numerical calculations. Further simplification of the equations in Sec. IIID is not possible without additional assumptions and, thus, numerical techniques must still be employed to obtain a complete solution even in the simplified case. However, if one can make a further assumption that the ion concentrations x_1 and x_2 are constant across the arc, a complete uncoupling of the equations is possible. Such an approximation might be reasonable, for instance, in a temperature range in which either single or double ionization was essentially complete, the other being negligible. Under this assumption we have from Eqs. (3.66) and (3.67)

$$\ell_a^{-1} = \frac{m_o}{\rho_{\ell_a} k_B (1+x_1+2x_2)} \int_o^1 \frac{P(\xi)}{T(\xi)} \, d\xi . \qquad (4.13)$$

Since Eq. (4.10) gives the temperature in the arc everywhere except for a negligible contribution near the boundaries, this expression may be used for T in Eq. (4.13) and we have, after employing Eq. (4.3) as well,

$$\frac{1}{\ell_a} = \frac{\mu j^{3/2} m_o}{\rho_{\ell_a} k_B (1+x_1+2x_2)} \left(\frac{64\lambda_o \sigma_s \sigma_o}{3} \right)^{\frac{1}{4}} \int_o^1 \frac{\xi - \xi^2/2}{\xi^{\frac{1}{2}} (5-2\xi)^{\frac{1}{4}} (1-\xi)^{\frac{1}{4}}} \, d\xi . \qquad (4.14)$$

The integral on the right-hand side of Eq. (4.14) is a constant independent of any properties of the arc and its value is about 0.46.

The value of ℓ_a for any particular set of input parameters can be calculated from Eq. (4.14) and results substituted into all equations in this section which depend on ℓ_a. Consequently, under these admittedly restrictive conditions, explicit values for all unknowns discussed in Sec. IIID can be obtained.

B. Numerical Solution.

The equations in Sec. IIID have been written in a form which makes them particularly amenable to solution by iterative techniques. Before proceeding, however, expressions for the conductivity σ and radiation mean free path λ are required. For the conductivity we have used a result obtained by Spitzer and coworkers[16-18] for a completely ionized gas, namely,

$$\sigma(\xi) = \frac{2.63 \times 10^{-2} \gamma_E T^{3/2}}{Z} \left[\log\left(\frac{1.23 \times 10^{7} T^{3/2}}{Z\sqrt{n_e}} \right) \right]^{-1} . \qquad (4.15)$$

Here Z, given by

$$Z = \frac{x_1 + 4x_2}{x_1 + 2x_2} , \qquad (4.16)$$

is a position-dependent number, lying between 1 and 2, which gives an indication of the degree of ionization in the gas. The multiplicative factor, γ_E, actually depends weakly on Z. For the problem at hand, however, the gas is nearly completely doubly ionized and γ_E can be well approximated by the value 0.6833.

An expression for the radiative mean free path averaged over the frequency spectrum (Rosseland mean free path) has been derived by Raizer[19] for a multiply ionized plasma. The derivation is based on the assumption that the atoms and ions which constitute the gas can be approximated by hydrogenic atoms or ions with an appropriate charge; it accounts for both bound-free and free-free (bremsstrahlung) transitions. One finds

$$\lambda(\xi) = \frac{0.91 \times 10^{11} k_B T^3 (1 + x_1 + 2x_2)}{P\left[(1 - x_1 - x_2) e^{-I_1/k_B T} + 4x_1 e^{-I_2/k_B T} + 9x_2 e^{-I_3/k_B T} \right]} \qquad (4.17)$$

for the case in which the gas is at most doubly ionized.

16. L. Spitzer, Physics of Fully Ionized Gases (Interscience, New York 1965), Chap. 5.
17. R.S. Cohen, L. Spitzer, and P. McR.Routly, "The Electrical Conductivity of an Ionized Gas", Phys. Rev. 80, 230 (1950).
18. L. Spitzer and R. Harm, "Transport Phenomena in a Completely Ionized Gas", Phys. Rev. 89, 977 (1953).
19. Y.P. Raizer, "Simple Method for Computing the Mean Range of Radiation in Ionized Gases at High Temperatures," Sov. Phys. - JETP 37, 769 (1960). See also Ref. 13, Chap. 5.

The numerical solution of the equations in Sec. IIID was then carried out as follows. The interval $0 \leq \xi \leq 1$ was divided into a few hundred equally spaced segments, and values for the position-dependent unknowns were estimated at every grid point from the approximate solution in Sec. IVA. Values for the constants ℓ_a and E_o were also estimated in this manner and a was calculated from Eq. (3.30). The estimated values were then used as initial values in an iterative technique by substituting them on the right-hand side of Eqs. (3.61) - (3.72) and calculating new values on the left-hand side. All integrals were evaluated simply by the trapezoidal rule. For the second iteration, a weighted average of the old and new values was used on the right-hand side. The process was then repeated and successive values were found to differ by only about one part in 10^4 after a few hundred iterations. Calculations were performed using different step sizes and it was found that approximately 400 grid points gave sufficiently accurate results. To the extent possible the mechanics of the program was checked using the analytic solution in Sec. IVA.

C. Application to Rashleigh-Marshall Experiment.

As pointed out in Sec. I, Rashleigh and Marshall[1] have used an arc-driven rail gun to accelerate a 3g mass to a velocity of about 6 km/s. We now wish to solve the equations in Sec. IIID using data appropriate to the RM experiment and, thereby, to analyze the arc. With two exceptions, the data which are listed in Table II are available either directly from the experiment or can be easily calculated therefrom. It has been necessary, however, to estimate the arc mass since this quantity was not measured experimentally and we have chosen to use the value of 0.1g estimated by McNab[7] in his earlier calculations. We have in subsequent work varied m_a, holding the other parameters fixed, and these results will be discussed in Sec. IVD. In addition, in the experiment the outer-most edges of the rails were surrounded by insulating material which excluded the arc from this region. Consequently, the rail height, h_r, was somewhat larger than the arc height measured along the rails, h_p. In the model studied here, both these heights were assumed equal and we have therefore used for h an effective height found from the geometric mean of the two values. The remaining quantities in the table are largely self-explanatory. The potential V_o is the voltage measured across the muzzle of the gun; it gives rise to the electric field in Eq. (3.21) and, since B=0 at the muzzle, it represents physically a purely resistive drop across the plasma. The atomic mass m_o was easily found to be the value indicated for the copper arc used in the experiment.

TABLE II. Experimental Data for Rashleigh-Marshall Experiment. The data, taken mostly from Ref. 1, were used in the numerical solution of the governing equations in Sec. IIID.

Quantity	Description	Value
w	Rail separation	1.27×10^{-2} m
h_p	Plasma height on rails	1.27×10^{-2} m
h_r	Rail height	1.91×10^{-2} m
h	Effective rail height	1.56×10^{-2} m
m_p	Projectile mass	3×10^{-3} kg
i	Pulsed current	3×10^{5} A
j	Current per unit height on rails	1.92×10^{7} A/m
V_o	Muzzle voltage	160 V
m_a^*	Arc mass	10^{-4} kg
m_o	Ion (or atom) mass	1.1×10^{-25} kg
a	Average acceleration	6×10^{6} m/s^2
ρ_{ℓ_a}	[See Eq. (3.29)]	0.51 kg/m^2
ρ_{ℓ_p}	[See Eq. (3.29)]	15.1 kg/m^2

* Estimated value.

The equations in Sec. IIID have been solved in the manner discussed in Sec. IVB and using the data in Table II. Results for the position-independent unknowns are indicated in Table III, while graphs of position-dependent quantities are shown by the solid-line curves in Figures 3-10. (The curves denoted by x's will be discussed in Sec. IVE.) These variables are plotted as a function of the dimensionless distance ξ. The brackets on quantities in Table III indicate that these variables were averaged over the length of the arc.

The value obtained for the acceleration is about a factor of two higher than the experimental value in Table II. Since a is a sensitive function of j, however, close agreement cannot be expected in view of the rather arbitrary manner in which h was chosen. The length of the

TABLE III. Results of Numerical Calculation for RM Experiment. The arc mass, m_a, was 0.1g.

Quantity	Value
a	1.48×10^7 m/s^2
ℓ_a	9.20 cm
E_o	3.72×10^3 volts/m
$< T >$	5.61×10^4 °K
$< Z >$	1.93
V_o	47 volts
$< n_e >$	9.85×10^{25} m^{-3}

arc ℓ_a was not explicitly measured in the experiment, but the calculated value is consistent with the estimate of around 10 cm.

The mean temperature is probably somewhat high, and it is likely that the high value results from the one-dimensional character of the model in which energy has been allowed to radiate only from the ends of the arc, not from the sides. In a two-or-three-dimensional model more surface area is available for radiation and the temperature must fall. A crude estimate of the mean temperature in a three-dimensional model may be obtained as follows. In one dimension, the surface area available for radiation is

$$A_1 = 2hw \ , \tag{4.18}$$

while in three dimensions one has

$$A_3 = 2\ hw + 2\ \ell_a\ w + 2\ \ell_a\ h \tag{4.19}$$

Using data for the RM experiment and assuming negligible change in ℓ_a, we find $A_3/A_1 \approx 14$. Since for a blackbody, the temperature varies inversely as the fourth root of the available surface area, we might expect a drop in $< T >$ of about a factor of two.

The average of the parameter Z, defined in Eq. (4.16), is included in the table in order to give some indication of the degree of ionization in the arc. Evidently, most of the ions are doubly ionized with very few singly ionized atoms in most of the arc. The high degree of second ionization makes it likely that some triple ionization, not accounted for, probably also exists. Again, however, Z should be considerably less in a two- or three-dimensional model because of the lower temperature.

Finally, the muzzle voltage which is easily calculated from the relation

$$V_o = E_o w \qquad (4.20)$$

was found to be 47 volts, about a factor of three smaller than that measured in the experiment. At the lower temperatures expected in three dimensions, V_o should increase since, according to Eq. (4.15), the conductivity of the arc decreases with decreasing T.

We see therefore that the calculated quantities which can be compared to the experimental results agree to within about a factor of three. The agreement, we feel, is reasonable in view of the restrictive assumptions made in the model as well as the arbitrary way in which m_a and h were obtained.

Plotted in Figure 3 is the pressure as a function of position in the arc. The pressure rises from zero at the trailing edge of the arc (a possible definition of the trailing edge) to a value at the projectile sufficient to provide an acceleration a, namely, $\rho_{\ell_p} a$. For the appropriate data, this value is roughly 220 MPa, or about 2200 atmospheres. If the current density in the arc were uniform, P would vary as $\xi - \xi^2/2$ (see Sec. IVA). The nonconstant current density, however, gives rise to deviations from this type of behavior observed in the graph. Similarly, the magnetic induction field, B, shown in Figure 4, varies from about 24 T at the trailing edge to zero at the projectile. The variation would be linear for constant current density as can be seen from Eq. (4.2).

The asymmetric nature of the temperature profile, shown in Figure 5, results from the position dependence of the radiation mean free path. Specifically, toward the leading edge of the arc where the density increases, the mean free path decreases. Consequently, photons created in the right-most part of the arc are radiated away with more difficulty than those in the left-most part, and there is a high concentration of energy near the projectile. Very near the projectile the temperature drops suddenly as was predicted by the analytic results in Sec. IVA.

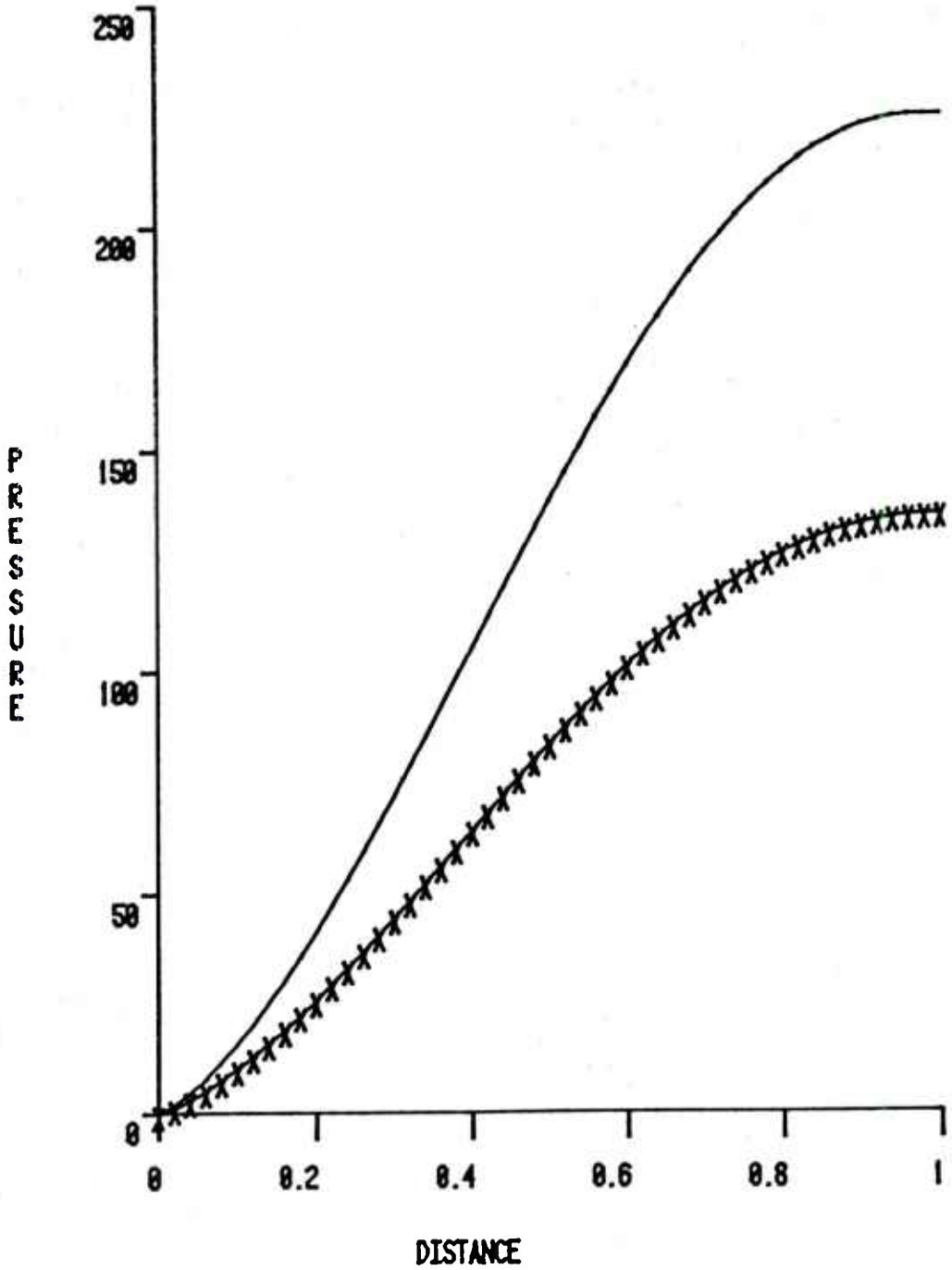

Figure 3. Pressure, in MPa, as a function of position in the arc: ————, calculation in Sec. IVC; xxx, calculation in Sec. IVE.

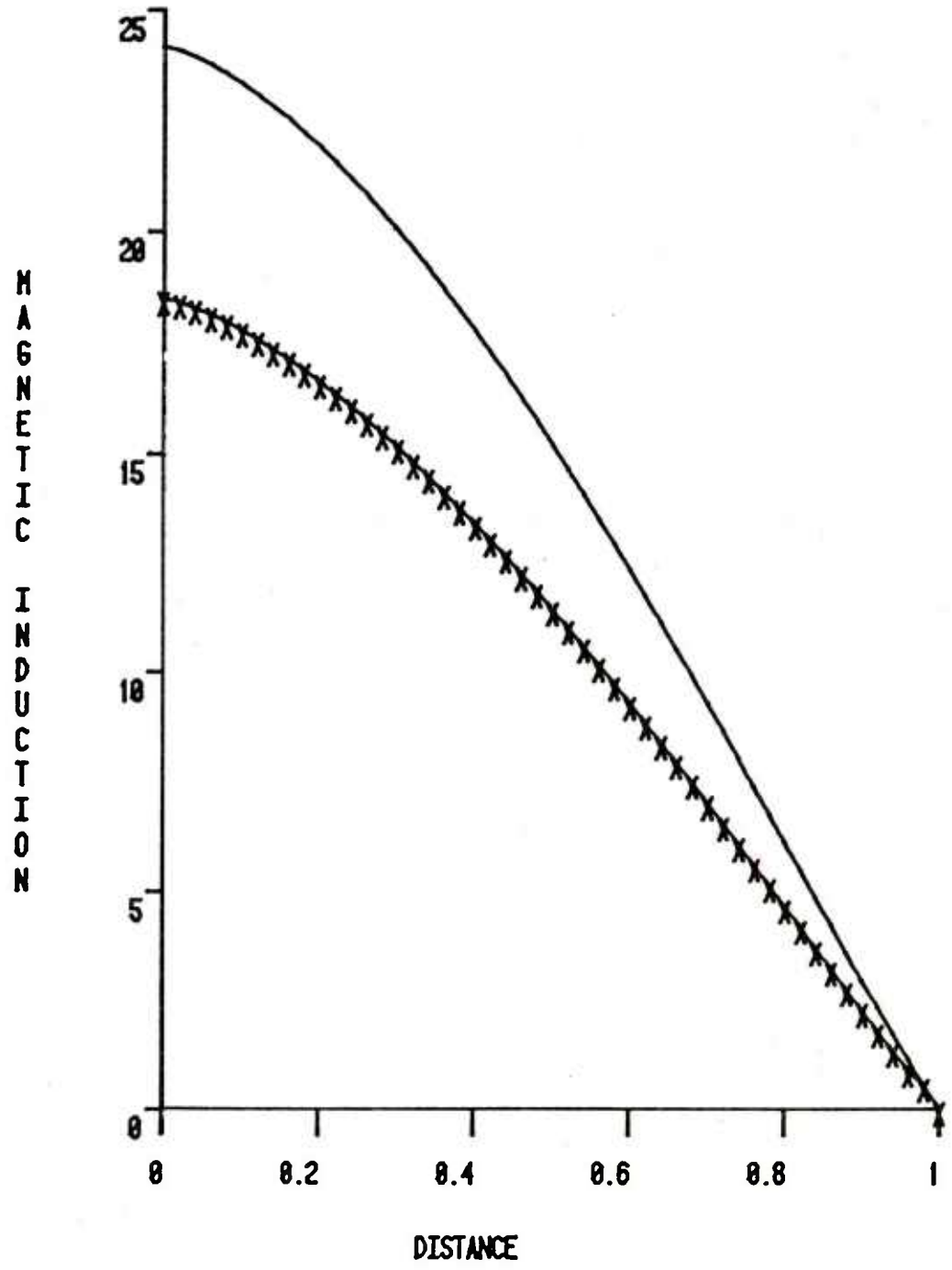

Figure 4. Magnetic induction field, in Tesla, as a function of position in the arc: ———, calculation in Sec. IVC; xxx, calculation in Sec. IVE.

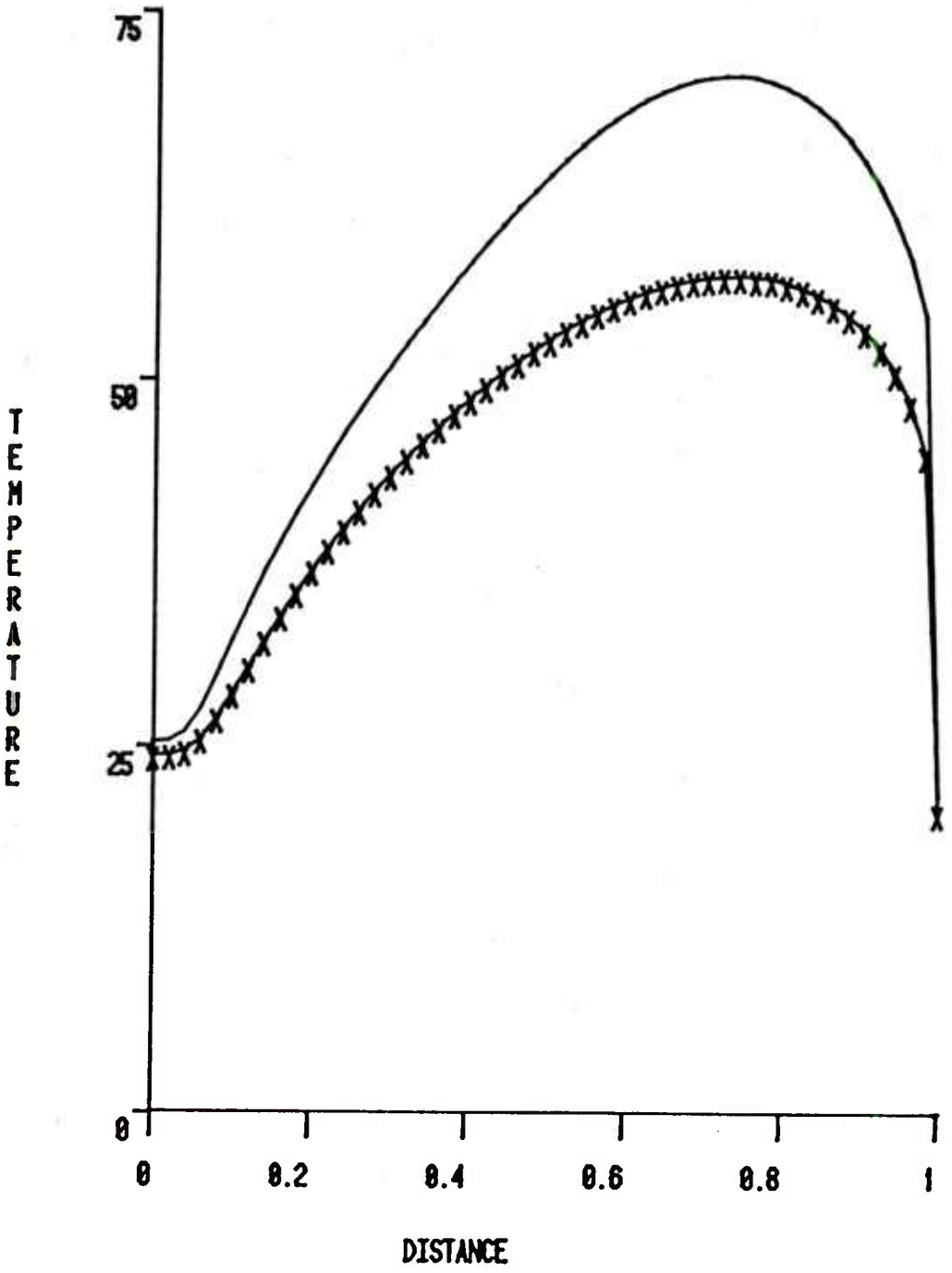

Figure 5. Temperature, in thousands of degrees Kelvin, as a function of position in the arc: ———, calculation in Sec. IVC; xxx, calculation in Sec. IVE.

Clearly once the photons are within a mean free path or so of the projectile surface, they are able to "see" the boundary and are radiated outward with little difficulty. Consequently, the temperature drops dramatically over this very short distance. It is also interesting to note that the temperature at $\xi = 0$, 2.53×10^4 °K, is larger than that at the projectile, 2.16×10^4 °K, by a factor of about 1.17. This factor is very close to that predicted by Eqs. (4.11) and (4.12), namely, $(5/3)^{1/4} \approx 1.14$.

The mass density, ρ, shown in Figure 6, varies nearly linearly from the expected value of zero at the trailing edge to about 10 kg/m^3 (about eight times the density of air at STP) at the leading edge. Very near the boundary a sudden rise in the density by about a factor of five is observed. The rise results because as the temperature drops at the boundary, the degree of ionization also drops, and both these effects tend to reduce the pressure near the projectile. Thus, a steady pressure at the projectile can be maintained only if there is a proportionate increase in mass density at the surface.

In Figure 7 is plotted the electron density, n_e, which varies in much the same manner as the mass density as should be expected. The rise near the projectile surface, however, is not so rapid as for the mass density; even though there are more ions near the boundary, they are less highly ionized than those interior to the arc because of the lower temperature.

The curve for the current density, J, shown in Figure 8, is largely self-explanatory. The current falls to zero at the trailing edge of the arc where the electron density is zero, increases with increasing temperature across the arc as should be expected from Eq. (4.15), and finally drops as T drops near the boundary. It should perhaps be noted from Eq. (4.15) that σ varies nearly as $T^{3/2}$, depending only weakly on the remaining parameters. (Z is nearly constant over most of the arc as can be seen in Figure 9.)

In Figure 9 is shown the mean ionic charge, Z, defined in Eq. (4.16). Except very close to the projectile, we found that essentially all the atoms in the arc were at least singly ionized with very few neutrals present. Therefore, within the arc a value of $Z = 2$ corresponds to $x_1 = 0$ and $x_2 = 1$, while a value of $Z = 1.8$ corresponds roughly to $x_1 = 0.33$, $x_2 = 0.67$. The unusual behavior of Z near the trailing edge of the arc results from the factor 1/P in the Saha equation. This dependence reflects the fact that electron reattachment is a two-body interaction, whereas ionization does not necessarily require a collision. However, the results are dependent on the assumption of thermal equilibrium which

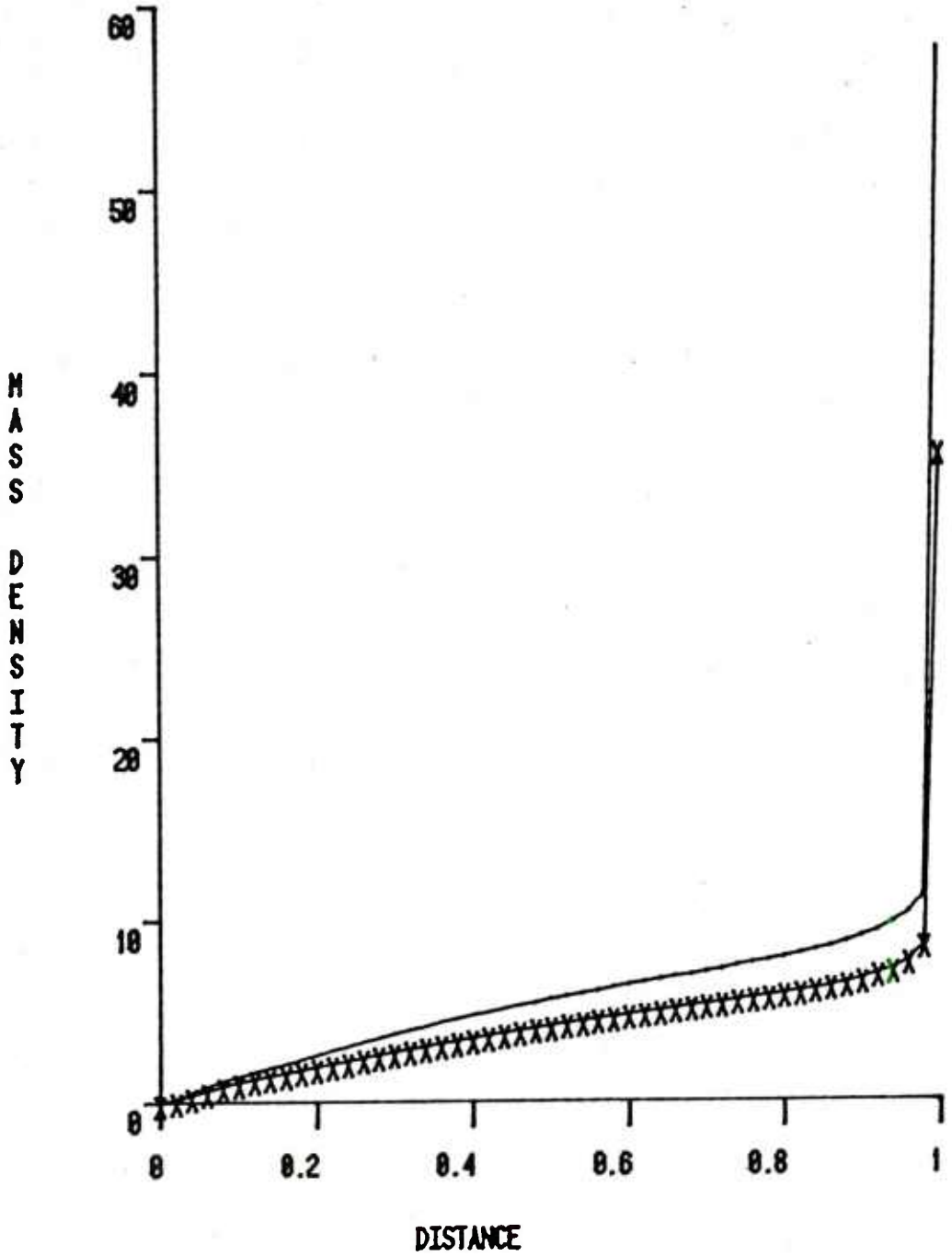

Figure 6. Mass density, in kg/m^3, as a function of position in the arc: ———, calculation in Sec. IVC; xxx, calculation in Sec. IVE.

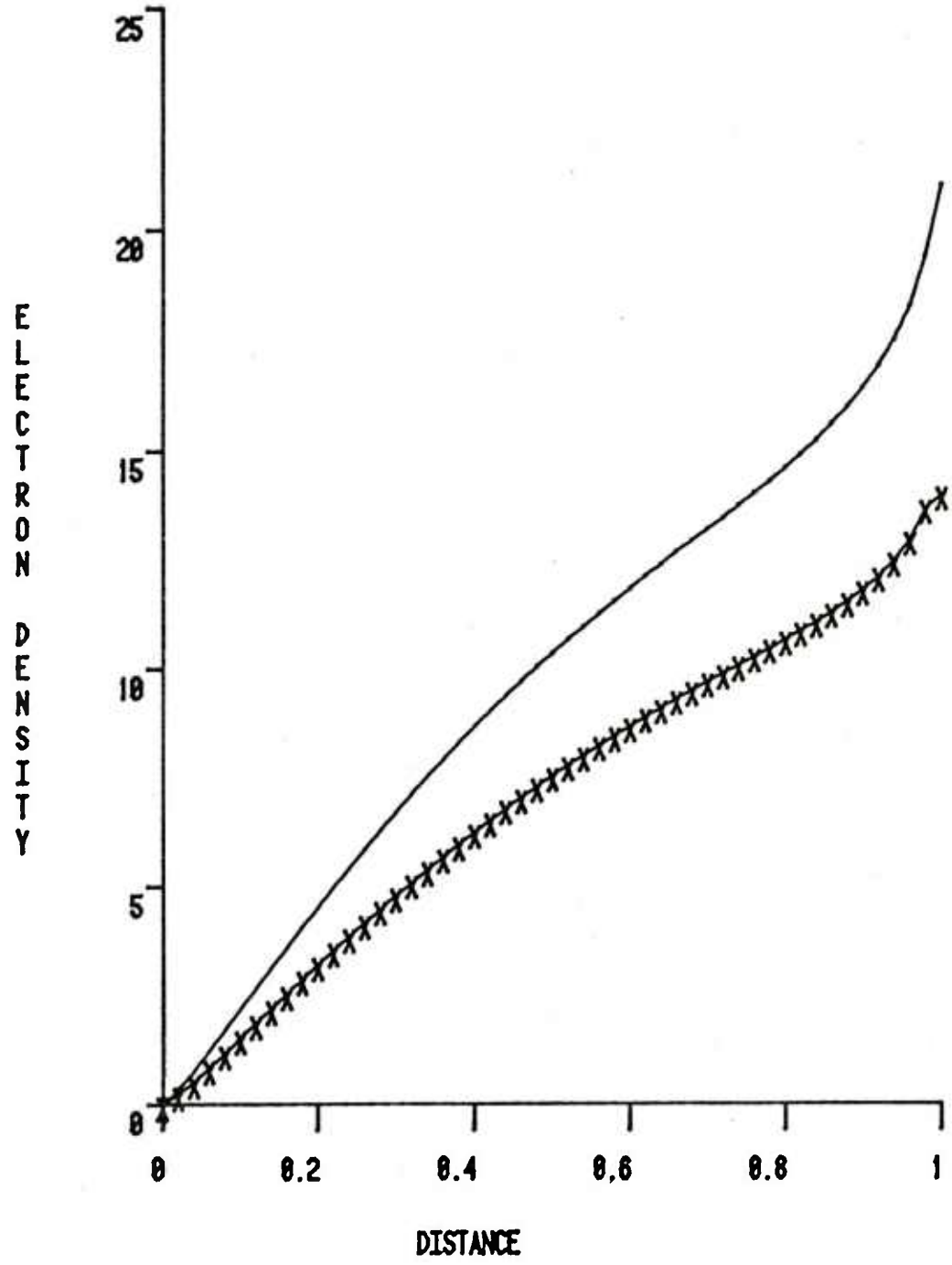

Figure 7. Electron density, in m^{-3} and normalized by the constant factor 10^{25}, as a function of position in the arc: ———, calculation in Sec. IVC; xxx, calculation in Sec. IVE.

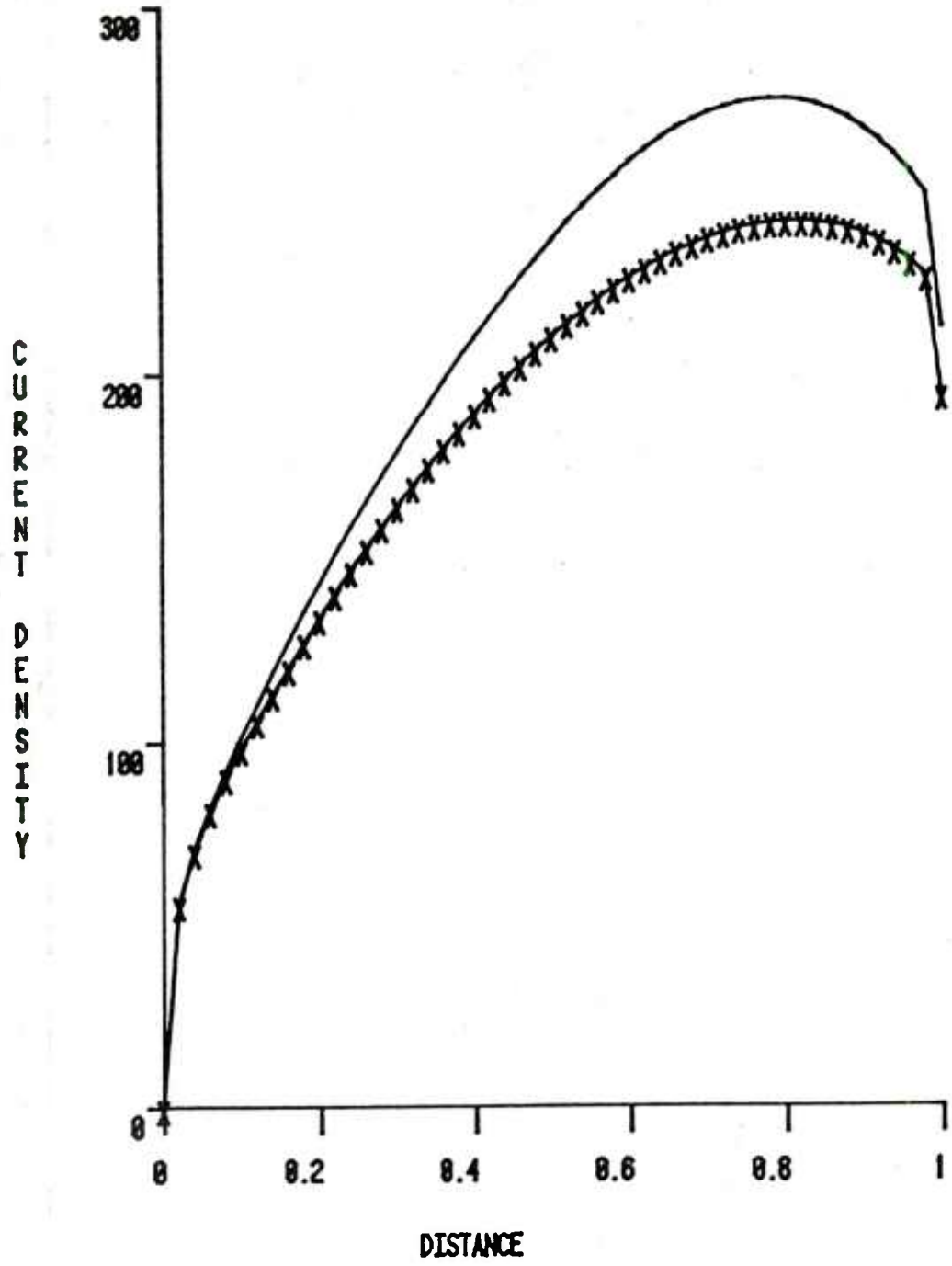

Figure 8. Current density, in MA/m^2, as a function of position in the arc: ———, calculation in Sec. IVC; xxx, calculation in Sec. IVE.

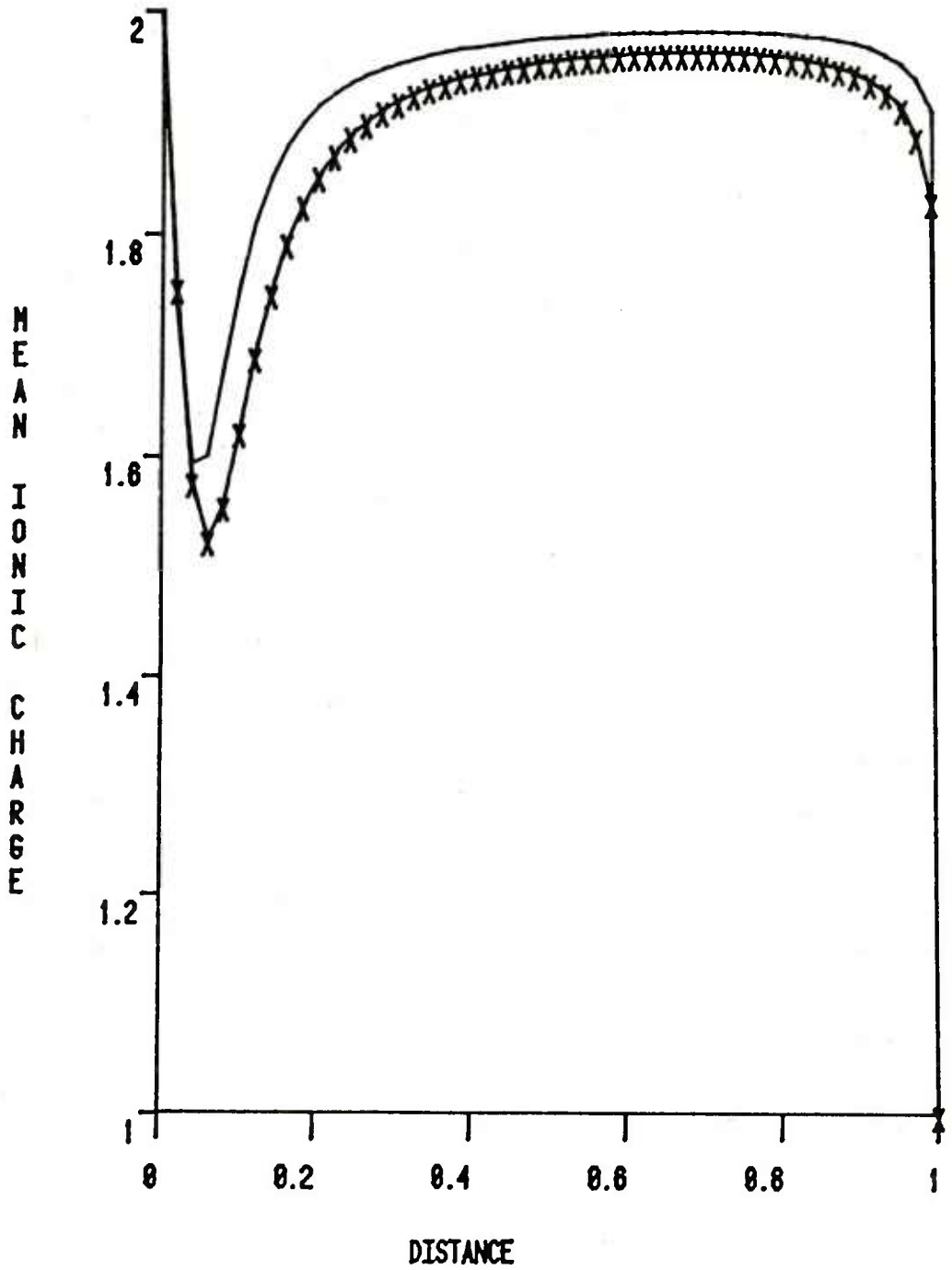

Figure 9. Mean ionic charge as a function of position in the arc: ———, calculation in Sec. IVC; xxx, calculation in Sec. IVE.

is not valid near $\xi=0$, owing to the small density there. Therefore, the detailed behavior of Z (and the other parameters) very near $\xi=0$ is probably open to question. In any case, the region in doubt is only a small portion of the overall profile and should have little effect on the mean properties and overall dynamics of the arc as suggested previously. Slightly to the right of $\xi=0$, the degree of ionization is determined predominantly by the temperature and increases with increasing temperature across the arc. Very near the projectile, the temperature drops dramatically with only a small variation in the pressure, so Z likewise drops. In fact, at the projectile surface, $x_1 = 0.38$ and $x_2 \approx 0$ so only 38% of the heavy particles which constitute the arc are at all ionized.

Finally, we show in Figure 10 the radiation heat flux q. For the limiting-case analytic solution, we found [see Eq. (4.8)], a linear behavior in q as a function of ξ with the flux changing sign at $\xi \approx 5/8 \approx 0.63$. For the more general calculation, the behavior is fairly well approximated by a linear variation and the sign changes around $\xi=0.72$.

D. Dependence of Results on Arc Mass.

Since it was necessary to estimate the value of the arc mass in the previous section, it is of some interest to ask how the results depend on m_a. We have therefore performed the calculation for a number of different values of m_a, holding the remaining parameters fixed at the values in the previous section.

Typical of the results are those shown in Table IV which are for an arc mass, m_a, of 0.05 g. As can be seen from the table, the acceleration of the arc is very slightly higher than before because of the de-

TABLE IV. Variation of RM Results With Arc Mass. Results were obtained using imput data in Table II, except that m_a was given by 0.05g.

Quantity	Value
a	1.51×10^7 m/s^2
ℓ_a	4.54 cm
E_o	7.47×10^3 volts/m
$\langle T \rangle$	5.66×10^4 °K
Z	1.94
V_o	95 volts
$\langle n_e \rangle$	1.00×10^{26} m^{-3}

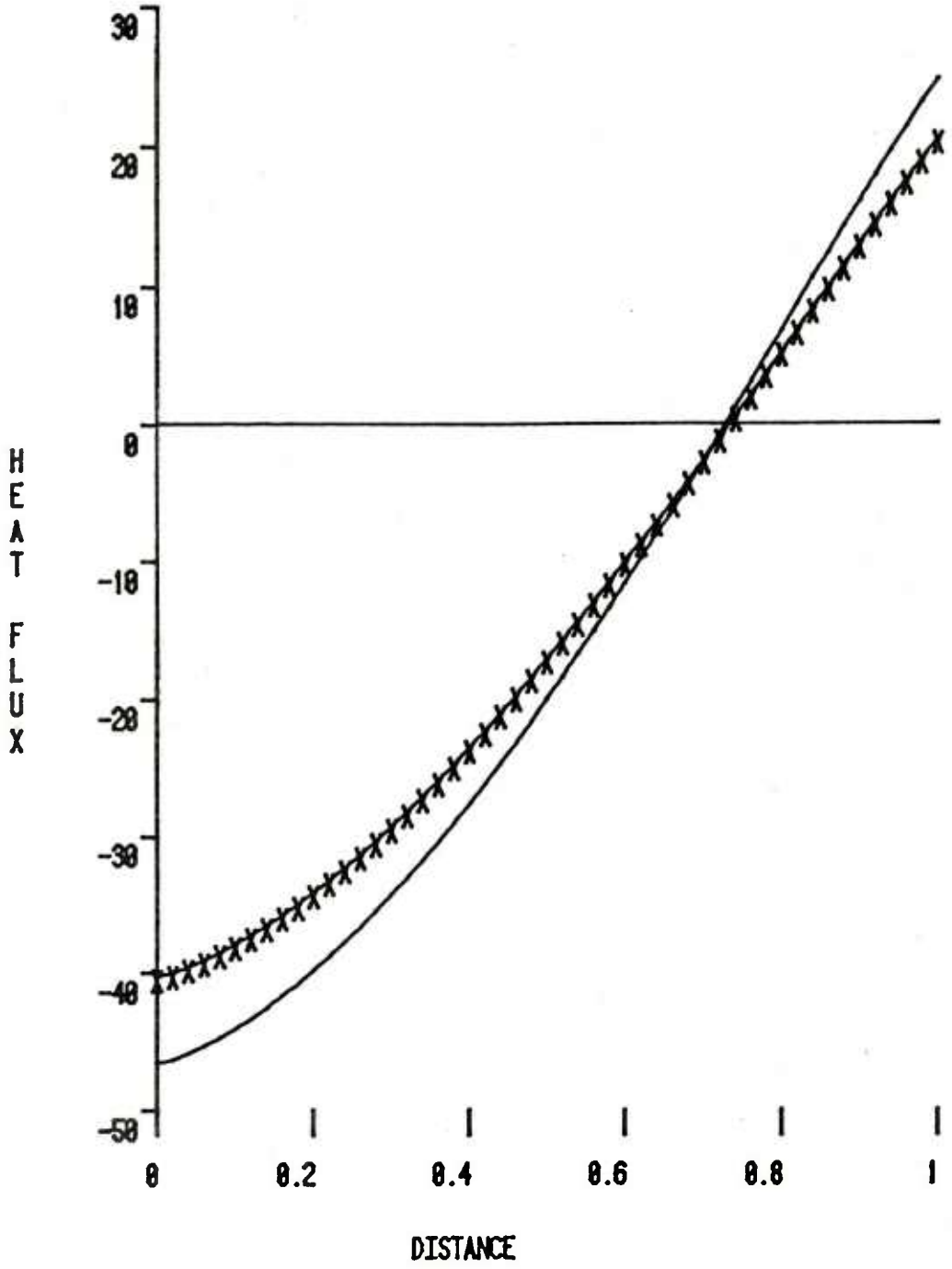

Figure 10. Heat flux, in $\frac{GJ}{s\ m^2}$, as a function of position in the arc: ———, calculation in Sec. IVC; xxx, calculation in Sec. IVE.

crease in the mass of the arc. Primarily the acceleration is determined by the more massive projectile, however, and the arc mass has only a minimal effect. The length of the arc has decreased by approximately a factor of two as might be expected intuitively. With the decrease in ℓ_a, E_o and consequently V_o rise by about a factor of two resulting from the increase in resistance of the arc. Likewise, the current density J in the arc, though not shown in the table, is everywhere higher by about a factor of two, owing to the decreased area of the arc.

It is noteworthy that, within the interior of the arc, the remaining position-dependent variables considered previously (B,P,T,ρ,n_e,x_1, and x_2) depend only very weakly on m_a when plotted as a function of the dimensionless distance ξ. In fact, when m_a was changed from 0.1 g to 0.05 g we observed changes of, at most, a few percent across the interior of the arc, though more significant changes did occur very near the boundaries. Except for the temperature, this result is perhaps not too surprising. It does appear, however, that the higher rate of energy dissipation in the smaller arc would surely result in a higher temperature. The reason for the unexpected result is that, even though the Joule heating is indeed greater in the smaller arc, so are the temperature gradients across the arc. Therefore, although energy is dissipated at a higher rate, it is also radiated away more easily. For the one-dimensional model under study here, the two effects almost exactly compensate each other so the arc seeks nearly the same steady-state temperature in the two cases. This, incidentally, will probably <u>not</u> be the case in a two- or three-dimensional model and one expects the temperature to rise with decreasing m_a (or ℓ_a).

The manner in which the parameters discussed above vary with ℓ_a can be seen approximately from the special-case solution in Sec. IVA. Thus, one sees from Eqs. (4.2) and (4.3) that B and P do not vary with m_a as a function of ξ. From Eq. (4.14), on the other hand, ℓ_a varies directly with m_a (or ρ_{ℓ_a}) in this limiting case and, therefore, as m_a decreases by a factor of two, so does ℓ_a. In accordance with Eq. (4.1), then, J should vary inversely with m_a as should E_o and V_o. T, on the other hand, is nearly independent of ℓ_a or m_a within the interior of the arc [Eq. (4.10)] but some variation can be expected very close to the boundaries [Eqs. (4.11) and (4.12)]. Finally, since ρ, x_1, and x_2 depend only on P and T, one expects them also to vary significantly with m_a only very near the boundaries.

Of course, the variations predicted by the limiting-case solution are only approximate in view of the assumptions made in obtaining that

solution. It is interesting, nevertheless, that the approximate scaling laws predicted from results in Sec. IVA appear to hold very nearly even for solutions to the more general equations.

E. Application to the Proposed Westinghouse Experiment and Scaling Factors.

We have also undertaken calculating the properties of the arc in a gun of the size proposed for the Westinghouse experiment. In particular, the input data for that calculation are shown in Table V. The rail gap, rail height, and projectile mass were chosen to be values appropriate for the proposed experiment; the value of the pulsed current i was chosen so as to provide an acceleration sufficient to reach a velocity of 3 km/s in a distance of 4m; and the arc mass was selected, mostly by trial and error, to give an arc length of the order of 10 cm.

TABLE V. Input Data for Large Gun. These data were used in the numerical solution of the governing equations in Sec. IIID; they correspond roughly to a gun comparable in size to that proposed in the Westinghouse experiment

Quantity	Description	Value
w	Rail separation	5×10^{-2} m
h	Rail height	5×10^{-2} m
m_p	Projectile mass	0.3 kg
i	Pulsed current	7.35×10^{5} A
j	Current per unit height on rails	1.47×10^{7} A/m
m_a	Arc mass	8×10^{-4} kg
ρ_{ℓ_a}	[See Eq. (3.29)]	0.32 kg/m^2
ρ_{ℓ_p}	[See Eq. (3.29)]	120 kg/m^2

General results of the numerical calculation are shown in Table VI and, as can be seen, quantities are of the same order of magnitude as obtained in the RM calculation. The largest difference in the two sets of data occurs for the potential across the rails which is larger than that for the RM experiment (with $m_a = 0.1$g) by nearly a factor of five. The higher value in the present case results from the higher current and higher arc resistance in the larger gun.

Table VI. Results of Numerical Solution for Large Gun. Input data used in the calculation are given in Table V.

Quantity	Value
a	1.13×10^{6} m/s^2
ℓ_a	7.82 cm
E_o	4.14×10^{3} volts/m
$< T >$	4.68×10^{4} °K
$< Z >$	1.89
V_o	207 volts
$< n_e >$	7.11×10^{25} m^{-3}

Graphs of position-dependent quantities are denoted for this calculation by the curves drawn with x's in Figures 3-10. The general discussion of the curves for the RM experiment applies here as well, and no further discussion will be given.

It is of interest to ask whether we can determine some approximate scaling laws from the analytic solution in Sec. IVA and, if so, to what extent these laws predict the results obtained for the larger gun. Fairly simple scaling laws can be derived from the analytic solution provided we make three additional assumptions: First, we assume that the degree of ionization does not appreciably change from one experiment to the other as can be seen to be the case for the RM and Westinghouse experiments. Second, we neglect the variation of the logarithmic term in Eq. (4.15), i.e., assume $\sigma \propto T^{3/2}$. Finally, we note that, for constant ionization, λ in Eq. (4.17) varies approximately as $T^{7/2}/\rho^2$. [19] If we make use of these assumptions, some simple algebra yields the scaling laws shown in Table VII. The pertinent equations for deriving the appropriate scaling factor are indicated in the right-most column of the table. To use the table, the value of a particular quantity in the RM experiment (column 1) is multiplied by the ratio of scaling factors for the large gun and RM gun. The numerical value of this ratio for the two experiments is shown in column 3. The result is then the predicted value of the quantity for the larger gun.

Table VII. Approximate Scaling Factors. Scaling factors were derived from the limiting-case analytic solution in Sec. IVA.

Quantity	Scaling Factor	Value	Equations
ℓ_a	$\rho_{\ell_a}/j^{16/11}$	0.92	3.66,4.3,4.10, 4.14, 4.15
a	$j^2/(\rho_{\ell_a} + \rho_{\ell_p})$	0.076	3.64
V_o	$j^{18/11}w/\rho_{\ell_a}$	4.08	3.62,3.66,4.3, 4.10,4.14,4.15, 4.20
E_o	$j^{18/11}/\rho_{\ell_a}$	1.03	3.62,3.66,4.3, 4.10,4.14,4.15
B	j	0.77	4.2
P	j^2	0.59	4.3
J	$j^{27/11}/\rho_{\ell_a}$	0.84	3.66, 4.1,4.3, 4.10,4.14,4.15
T	$j^{6/11}$	0.87	3.66,4.3,4.10, 4.15
ρ	$j^{16/11}$	0.68	3.66,4.3,4.10, 4.15
n_e	$j^{16/11}$	0.68	3.66, 3.70, 4.3, 4.10,4.15
q	$j^{29/11}/\rho_{\ell_a}$	0.80	3.66,4.3,4.8, 4.10,4.14,4.15

Values obtained in this manner for the parameters in Table VI were: $a = 1.13 \times 10^6$ m/s^2, $\ell_a = 8.46$ cm, $E_o = 3.83 \times 10^3$ volts/m, $\langle T \rangle = 4.88 \times 10^4$ °K, $V_o = 192$ volts, and $\langle n_e \rangle = 6.70 \times 10^{25}$m^{-3}. As can be seen, values of the parameters obtained from the scaling laws agree with the actual theoretical values in Table VI to within, at worst, about 15%. We have also investigated the validity of the scaling laws in predicting the values of position-dependent quantities and, again, found reasonable agreement. Typical of the results is that shown in Figure 11. The curve denoted by the x's is the theoretical value of the arc temperature for the larger gun plotted as a function of ξ (see Figure 5); the curve denoted by the 0's is the same function but obtained from the scaling laws. The latter curve was deduced by multiplying the temperature at every point ξ in the RM experiment by the appropriate scaling factor, namely, 0.87. As can be seen the results agree everywhere to within less than 10%.

It appears, therefore, that no major difficulties should be encountered if it should be desirable to employ an arc in the proposed Westinghouse experiment. All properties of the arc are expected to be the same order of magnitude as for the RM experiment. Furthermore, approximate values of the pertinent parameters can be obtained from the scaling factors in Table VII.

V. DISCUSSION

In this final section, we will discuss the calculation briefly, particularly the major assumptions, indicate the limitations of the model, and suggest what future calculations might be desirable. To summarize, we have proposed a model for determining the steady acceleration of the arc and projectile in the arc-driven electric gun and for describing the fluid-mechanical properties of the arc. A set of twelve coupled equations has been derived which, when solved, yields these properties. The theory has been applied to the RM experiment as well as to the experiment proposed by Westinghouse. It has been demonstrated that use of an arc in the larger gun should pose no major obstacles.

As pointed out in Sec. I, some earlier analysis of arc dynamics in the RM experiment has been carried out by McNab[7]. He assumed that one-third of the measured muzzle voltage ($\approx$ 53 volts) occurred across the plasma and used this experimental value to calculate the temperature of the arc. The spatial variation of all flow parameters was neglected and the gas was assumed to be, at most, singly ionized. In addition, the experimental value of the acceleration was used in the calculation and the arc length was assumed to be 10 cm. Values obtained for the pressure, temperature, electron density, and arc mass were: P=110 MPa,

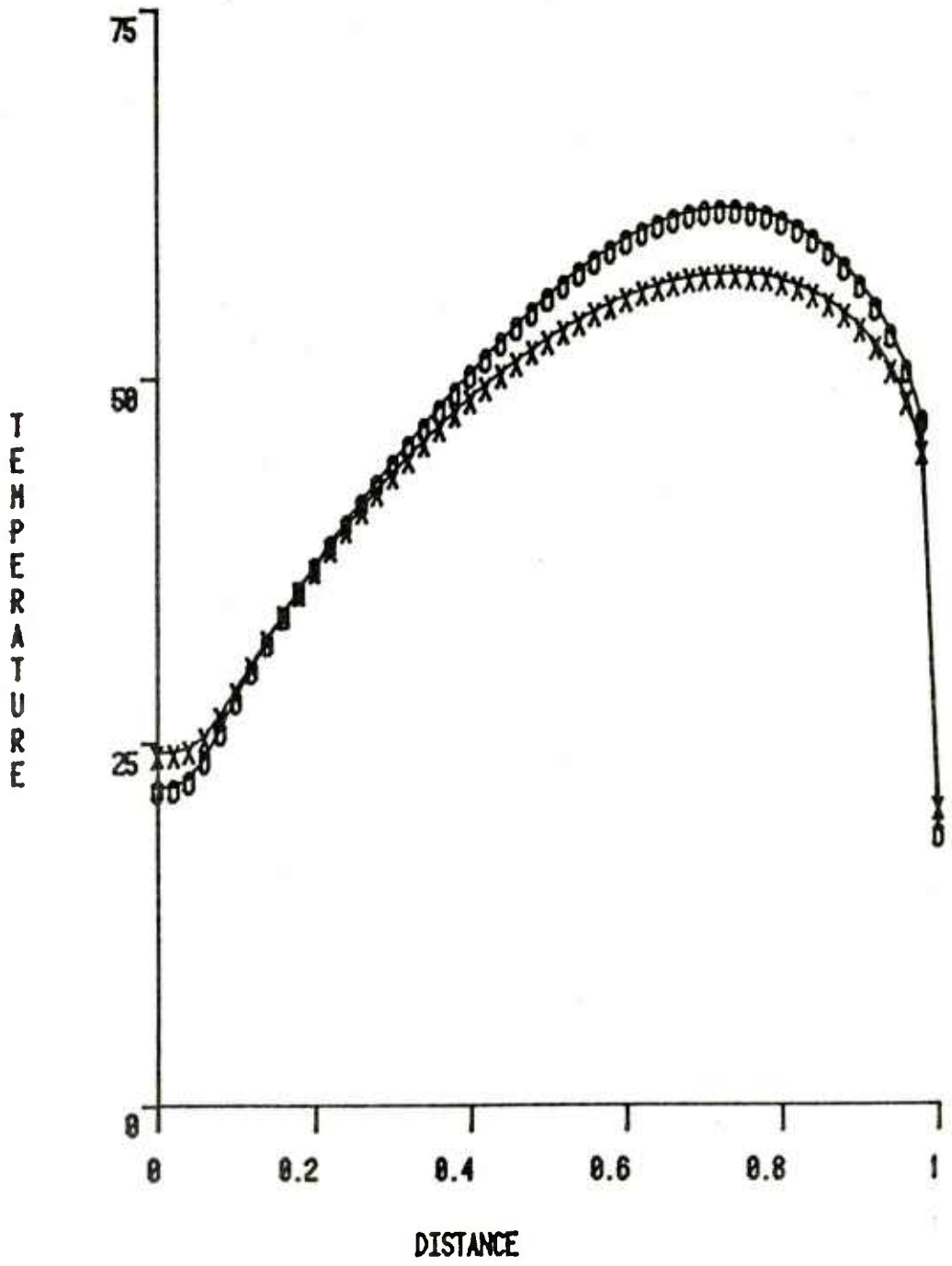

Figure 11. Comparison of numerical results of temperature profile with results obtained from scaling laws: xxx, numerical results from calculation in Sec. IVE; OOO, results obtained from scaling laws in Table VII.

$T = 5.7 \times 10^4$ deg, $n_e = 7 \times 10^{25} m^{-3}$, and $m_a = 0.1g$. Clearly, McNab's results are in order-of-magnitude agreement with results obtained in Sec. IVC.

The rationale for assuming that only one-third of the potential difference between the rails occurs across the arc is, as McNab pointed out, that some contact potential surely exists at the rail-arc interface. This contact potential has not been included in the present calculation primarily because it is not clear experimentally how significant a potential drop actually exists. Admittedly, however, the contact potential is probably not negligible and some further investigation is appropriate. Presumably, the effect could be included in the model with little additional difficulty.

The major assumption that has been employed in the present calculations is that the entire acceleration process can be approximated by conditions appropriate to the steady state. This approximation should be reasonable provided the time required for a steady state to be established is small compared to the total time of acceleration. Obviously, the validity of the approximation cannot be rigorously ascertained without, in fact, solving the time-dependent problem. Nevertheless, several necessary conditions might be mentioned.

First, it is clear that for the steady-state approximation to be valid, the current, which initially flows on the surface of the arc, must diffuse through it in a time small compared to the total acceleration time. Alternatively, the skin depth, δ, of the plasma must be large compared with its length. The skin depth of the plasma at time t can be estimated from the expression[20]

$$\delta = \left(\frac{\pi t}{\mu \sigma_o}\right)^{\frac{1}{2}} = \left(\frac{\pi t \ell_a V_o}{\mu j w}\right)^{\frac{1}{2}}, \qquad (5.1)$$

where σ_o here denotes the mean conductivity of the arc. The second equality in Eq. (5.1) follows from Eqs. (3.15) and (4.20) with J approximated by j/ℓ_a. For an acceleration time appropriate to the RM experiment, namely, 1.6 ms and assuming $V_o = 47$ volts, the theoretical value, we find, $\delta \approx 30$ cm. Clearly, δ is considerably larger than the arc length of 9.2 cm. That the skin depth here is larger than those generally associated with solid conductors results from the lower conductivity in the gaseous state.

20. W.R. Smythe, in American Institute of Physics Handbook, edited by D.E. Gray (McGraw-Hill, New York, 1957), p. 5-85.

A second condition which must be satisfied in order to justify the steady-state approximation is that the time required for the plasma to reach its steady-state internal energy must be small compared to the total acceleration time. The internal energy of the plasma at any time can be determined from the relation

$$E_{int} = E_T + E_i + E_e \tag{5.2}$$

where E_T, E_i, and E_e denote the thermal, ionization, and electronic energies, respectively, whereas the energy which has been dissipated in the arc at time t is given by

$$E_D = h\, w\, \ell_a t \int_0^1 \frac{J^2}{\sigma}\, d\xi = h\, w\, t\, E_o j\ . \tag{5.3}$$

Assuming that the gas is completely doubly ionized, a simple estimate reveals that for the RM experiment, $E_{int} \approx 6$ kJ. If we neglect losses in energy due to radiation during the time for which the plasma is being heated, the time required for the plasma to reach its steady internal energy can be found by substituting E_{int} on the left-hand side of Eq. (5.3) and solving for t. We find $t \approx 0.4$ ms, a value somewhat smaller than the total acceleration time of 1.6 ms. The assumption that radiation losses are negligible during the time of heating is probably reasonable, since the radiation flux varies as T^4. It is of interest to note, incidentally, that the total energy dissipated in the arc during the acceleration time of 1.6 ms is about 20 kJ. This energy is considerably less than the kinetic energy of the arc and projectile which is, using the theoretical value of the acceleration, about 870 kJ. In the model, the remaining energy supplied by the source is stored in the magnetic field, and it can be shown that this energy is identical to the kinetic energy of the arc and projectile.

Finally, a less stringent condition which must be satisfied in order to justify the steady-state approximation is that the time of acceleration must be large compared to the time necessary for a sound wave to traverse the arc. If this condition is not met, it is clear that the flow variables cannot become equilibrated during the time of acceleration, and that they will be time dependent in a frame accelerating with the arc. One can estimate, however, that the sound speed in the plasma is of the order of a few kilometers per second. Thus, the time necessary for a disturbance to traverse an arc 10 cm long is probably somewhat less than 10^{-4}s. Again, this is substantially less than the acceleration time of 1.6 ms.

The above considerations do not prove the validity of the steady assumption and further investigation is desirable. In principle, a time-dependent theoretical treatment, accounting for the the initial

compression and expansion of the arc and the diffusion of current within it, should be possible. Such a calculation, however, would be immensely more difficult than that undertaken here and would necessitate additional experimental data and assumptions. It would be necessary to know, for instance, the conditions of the arc prior to the time the acceleration begins and this information is not currently available. Probably so detailed a calculation is not justified considering our current state of experimental knowledge. In future experiments it would be desirable if investigators could measure the temperature of the arc by, for example, spectroscopic means. The adequacy of various theoretical treatments could then be ascertained and more sophisticated calculations undertaken.

Some of the remaining assumptions made in the model calculation merit some brief discussion. First, we found that over most of the arc essentially all of the ions were doubly ionized. The high degree of ionization suggests that some triple ionization is probably also present, and triple ionization is not accounted for. As has been pointed out, however, in a two- or three-dimensional model, one expects lower temperatures and, in that case, higher ionization is probably negligible. Account could be taken, of course, of triple ionization by including an additional equation in the hierarchy represented by Eqs. (3.53). The spectrum of trebly ionized copper has been reported in the literature[21], and so the calculation should be quite straightforward. In practice, however, the algebra becomes extremely tedious and is probably not justified in view of the rather limited improvements anticipated in the results.

The relative importance of ordinary heat conduction, neglected in the calculation, and radiation can be estimated by comparing the coefficient of thermal conductivity to the coefficient of radiation heat conduction. The latter coefficient is defined in Eq. (3.38), viz.,

$$\kappa_R = \frac{16\sigma_s \lambda\, T^3}{3}, \tag{5.4}$$

whereas the thermal-conductivity coefficient can at least be approximated by the expression appropriate for a Lorentz gas. One has[16]

$$\kappa_c = \frac{1.96 \times 10^{-9} T^{5/2}}{Z} \left[\log\left(\frac{1.23 \times 10^{7} T^{3/2}}{Z\sqrt{n_e}} \right) \right]^{-1} \tag{5.5}$$

21. J.M. Schroeder and Th. A.M. Van Kleef, "The Spectrum of Trebly Ionized Copper", Physica 49, 388 (1970).

and the ratio of the two values is

$$\frac{\kappa_R}{\kappa_c} = 1.5 \times 10^2 \lambda Z T^{\frac{1}{2}} \log\left(\frac{1.23 \times 10^7 T^{3/2}}{Z\sqrt{n_e}}\right). \qquad (5.6)$$

Radiation mean free paths, λ, in the calculation were found to be typically of the order of 10^{-4}m, and, assuming as approximate mean values, Z=2, T = 5.6×10^4 deg, $n_e = 10^{26}$ m^{-3}, we find $\kappa_R/\kappa_c \approx 15$. Thus, radiation is substantially more important than heat conduction for the case under study here. The small value of λ quoted above, incidentally, serves also to justify representing the radiation flux by Eq. (3.38). As pointed out in Sec. IIIB, the validity of that assumption depends on the condition $\lambda << \ell_a$.

It was also suggested in Sec. IIIB that the condition $\lambda << \ell_a$ should imply that the properties of the arc are nearly independent of the temperature at the projectile surface. This assertion was used to justify employing the boundary condition in Eq. (3.39) to determine the surface temperature. To check the validity of the assertion, we have performed the calculation holding the projectile surface at some different temperature and observed little change in the results. In fact, although we lowered the temperature at the surface by more than an order of magnitude from the value predicted in the original calculation, we observed negligible change in T within the interior of the arc. There was a substantial difference in the temperature within a mean free path or so of the boundary for the two calculations, but this difference is of little practical importance.

One of the least satisfactory aspects of the present calculation is the reliance on Eqs. (4.15) and (4.17) for the conductivity and mean free path for the arc. As pointed out, the derivation of Eq. (4.17) is based on the hydrogenic approximation and the resulting expression is probably accurate to within no better than an order of magnitude[19]. Furthermore, the theory used to develop Eq. (4.15) is known to break down for high electron densities and low temperatures. For the cases under study here, we are probably very near, if not beyond, the limit of validity of the theory. Experiments[22], however, have suggested that Eq. (4.15) may be more generally applicable than would be expected on purely theoretical grounds[16]. At any rate, future attempts to determine more accurate expressions for these quantities, or to establish more firmly the validity of existing ones, would be desirable.

22. S.C. Lin, E.L. Resler and A. Kantrowitz, "Electrical Conductivity of Highly Ionized Argon Produced by Shock Waves", J. Appl. Phys. 26, 95 (1955).

It may be mentioned, incidentally, that a modification to Eq. (4.15) has been derived[16,23] for the case in which conduction takes place normal to a strong magnetic field. The revised expression accounts for the tendency of the electrons to spiral in such a field, reducing the conductivity. Since the fields under consideration here are quite large, it might appear that the modified conductivity would be appropriate. It must be remembered, however, that the density is also quite large over most of the arc and, thus, the mean free path is small. Therefore, the spiralling effect is substantially reduced. Quantitatively, the condition which must be satisfied in order to use the high-field conductivity is that the electron gyration radius be small compared to its mean free path. Our estimates indicate, however, that the ratio of these two parameters is 10 or greater except very near the trailing edge of the arc. Therefore, the use of Eq. (4.15), without the high-field approximation, is justified. This point has been discussed further by McNab[7].

The foregoing discussion makes clear the need for some specific future studies. First, it would be worthwhile to extend the calculations to two or three dimensions. As pointed out previously, the one-dimensional model probably overestimates the temperature of the arc, and does not account for any spatial variation of the flow parameters in directions normal to the acceleration direction. In addition, use of infinitely high rails overestimates the inductance per unit length of the rails and is responsible, in part, for the relatively high theoretical value for the acceleration obtained in Sec. IVC. Second, some consideration of time-dependent effects would be worthwhile, if only to better justify the steady-state assumption. Third, it would be of interest to carry out the calculations for arcs other than the copper-vapor arc studied here. From such investigations we could determine how the properties of the arc material affect the overall arc dynamics and which arcs produce the most desirable effects. Finally, some effort should be expended to determine the amount of heat transferred to the rails. When compared to the results for more conventional guns, the analysis should provide a preliminary step in the study of gun-tube erosion for the rail gun.

ACKNOWLEDGMENT

We thank D. Eccleshall and A. Gauss for useful discussions.

23. L. Spitzer, "Equations of Motion for an Ideal Plasma", Astrophys. J. 116, 299 (1952).

REFERENCES

1. S.C. Rashleigh and R.A. Marshall, "Electromagnetic Acceleration of Macroparticles to High Velocities", J. Appl. Phys. 49, 2540 (1978).

2. R.A. Marshall, "The Australian National University Rail Gun Project", Atomic Energy, 16, January 1975.

3. J.P. Barber, "The Acceleration of Macroparticles and a Hypervelocity Electromagnetic Accelerator", Ph.D. Thesis (Australian National University, 1972) (Unpublished).

4. H. Kolm, "Basic Coaxial Mass Driver Reference Design", Third Princeton/AIAA Conference on Space Manufacturing Facilities, Paper No. 77-534, Princeton, NJ, May 1977.

5. K. Fine, "Basic Coaxial Mass Driver Construction and Testing", Third Princeton/AIAA Conference on Space Manufacturing Facilities, Paper No. 77-535, Princeton, NJ, May 1977.

6. D.E. Brast and D.R. Sawle, "Study of a Rail-Type MHD Hypervelocity Projectile Accelerator", Proc. Seventh Hypervelocity Impact Symposium, 1964, Vol. 1, p. 187 (unpublished).

7. I. McNab, "Electromagnetic Acceleration by a High Pressure Plasma", J. Appl. Phys. 51, 2549 (1980).

8. Authors' unpublished calculations.

9. R.M. Fano, L.J. Chu, and R.B. Adler, Electromagnetic Fields, Energy, and Forces (Wiley, New York, 1960), Chap. 9.

10. Authors' unpublished calculations.

11. A.B. Cambel, Plasma Physics and Magnetofluidmechanics (McGraw Hill, New York, 1963), Chap. 8.

12. J.D. Jackson, Classical Electrodynamics (Wiley, New York, 1962), Chap. 5.

13. Y.B. Zel'dovich and Y.P. Raizer, Physics of Shock Waves and High-Temperature Hydrodynamic Phenomena (Academic, New York, 1966), Vol. I, Chap. 2.

14. See Ref. 13, Chap. 3.

15. Data taken from C.E. Moore, "Atomic Energy Levels", National Bureau of Standards Circ. No. 467, V. II, Washington, DC, 1952.

16. L. Spitzer, Physics of Fully Ionized Gases (Interscience, New York, 1965), Chap. 5.

17. R.S. Cohen, L. Spitzer, and P. McR. Routly, "The Electrical Conductivity of an Ionized Gas", Phys. Rev. 80, 230 (1950).

18. L. Spitzer and R. Harm, "Transport Phenomena in a Completely Ionized Gas", Phys. Rev. 89, 977 (1953).

19. Y.P. Raizer, "Simple Method for Computing the Mean Range of Radiation in Ionized Gases at High Temperatures", Sov. Phys. - JETP 37, 769 (1960). See also Ref. 13, Chap. 5.

20. W.R. Smythe, in American Institute of Physics Handbook, edited by D.E. Gray (McGraw-Hill, New York, 1957), p. 5-85.

21. J.M. Schroeder and Th. A.M. Van Kleef, "The Spectrum of Trebly Ionized Copper", Physica 49, 388 (1970).

22. S.C. Lin, E.L. Resler and A. Kantrowitz, "Electrical Conductivity of Highly Ionized Argon Produced by Shock Waves", J. Appl. Phys. 26, 95 (1955).

23. L. Spitzer, "Equations of Motion for an Ideal Plasma", Astrophys. J. 116, 299 (1952).

APPENDIX

The purpose of this appendix is to prove the statement made in Sec. III that the acceleration of the arc and projectile is independent of how the current is distributed in the arc and is given by

$$a = \frac{\mu j^2}{2\left(\rho_{\ell_a} + \rho_{\ell_p}\right)} . \tag{A.1}$$

From Eqs. (3.5) and (3.29) we have

$$a = \frac{\mu \ell_a^2}{\rho_{\ell_a} + \rho_{\ell_p}} \int_0^1 J(\xi) \left[\int_\xi^1 J(\xi')\, d\xi' \right] d\xi . \tag{A.2}$$

Now define the function

$$u(\xi) = \int_\xi^1 J(\xi)\, d\xi \tag{A.3}$$

and differentiate to produce

$$\frac{du}{d\xi} = - J(\xi) . \tag{A.4}$$

Substituting Eqs. (A.3) and (A.4) into Eq. (A.2), we find

$$a = \frac{-\mu \ell_a^2}{\rho_{\ell_a} + \rho_{\ell_p}} \int_0^1 u \frac{du}{d\xi}\, d\xi , \tag{A.5}$$

whence

$$a = \frac{-\mu \ell_a^2}{2\left(\rho_{\ell_a} + \rho_{\ell_p}\right)} \left[u^2(1) - u^2(0) \right] . \tag{A.6}$$

However, according to Eq. (3.16), $u(0) = \frac{j}{\ell_a}$, whereas $u(1) = 0$, so

$$a = \frac{\mu j^2}{2\left(\rho_{\ell_a} + \rho_{\ell_p}\right)} . \tag{A.7}$$

DISTRIBUTION LIST

No. of Copies	Organization
12	Commander Defense Technical Info Center ATTN: DDC-DDA Cameron Station Alexandria, VA 22314
1	Office Under Secretary of Defense Res & Engr ATTN: Mr. Ray Thorkildsen Room 3D1089, Pentagon WASH, DC 20301
1	Deputy Under Secretary of Defense-Res & Engr ATTN: Dr. Arden L. Bement Room 3E144, Pentagon WASH, DC 20301
3	Director Defense Advanced Research Projects Agency ATTN: Dr. Joseph Mangano Dr. Gordon P. Sigman Dr. Raymond P. Gogolewski 1400 Wilson Blvd Arlington, VA 22209
1	Office of Assistant Secretary of the Army ATTN: RDA, Dr. Joseph Yang Room 2E672, Pentagon WASH, DC 20310
1	HQDA (DAMA-ARZ-A, Dr. Marvin Lasser) WASH, DC 20310
1	Commander US Army Materiel Development & Readiness Command ATTN: DRCDMD-ST 5001 Eisenhower Avenue. Alexandria, VA 22333
1	Commander US Army Materiel Development & Readiness Command ATTN: DRCLDC, Mr. T. Shirata 5001 Eisenhower Avenue Alexandria, VA 22333
7	Commander US Army Armament Research and Development Command ATTN: DRDAR-TSS (2 cys) DRDAR-LCA,Mr. J.A.Bennett DRDAR-LCA,Dr. H. Fair DRDAR-LCA,Dr. T. Gora DRDAR-LCA,Dr. P. Kemmey DRDAR-AC,COL R. Mathis Dover, NJ 07801
1	Commander US Army Armament Materiel Readiness Command ATTN: DRSAR-LEP-L, Tech Lib Rock Island, IL 61299
1	Director US Army ARRADCOM Benet Weapons Laboratory ATTN: DRDAR-LCB-TL Watervliet, NY 12189
1	Commander US Army Aviation Research & Development Command ATTN: DRSAV-E P.O. Box 209 St. Louis, MO 61366
1	Director US Army Air Mobility Research & Development Laboratory Ames Research Center Moffett Field, CA 94035

DISTRIBUTION LIST

No. of Copies	Organization
1	Commander US Army Communications Rsch & Dev Command ATTN: DRDCO-PPA-SA Fort Monmouth, NJ 07703
1	Commander US Army Electronics R&D Command Technical Support Activity ATTN: DELSD-L Fort Monmouth, NJ 07703
2	Commander US Army Missile Command ATTN: DRSMI-R DRSMI-YDL Redstone Arsenal, AL 35809
1	Commander US Army Tank Automotive Rsch & Development Command ATTN: DRDTA-UL Warren, MI 48090
1	Director US Army TRADOC Systems Analysis Activity ATTN: ATAA-SL, Tech Lib White Sands Missile Range, NM 88002
2	Commander US Army Research Office ATTN: Dr. Fred Schmiedeshoff Dr. M. Ciftan P.O. Box 12211 Research Triangle Park, NC 27709
1	Commander Naval Air Systems Command ATTN: Dr. Richard J. Wasneski Code 350F WASH, DC 20361
1	Commander US Naval Research Laboratory ATTN: Dr. Ihor Vitkovitsky, Code 4770 WASH, DC 20375
2	Commander Naval Surface Weapons Center ATTN: Henry B. Odom, Code F-12 Dr. M. Franklin Rose, Code F-04 Dahlgren, VA 22448
2	AFATL (Dr. Dale M. Davis, Virgil Miller) Eglin AFB, FL 32542
1	AFWL (Dr. William L. Baker) Kirtland AFB, NM 87117
1	AFAPL (Dr. Charles E. Oberly) Wright-Patterson AFB, OH 45433
1	Director Brookhaven National Laboratory ATTN: Dr. James R. Powell Bldg 129 Upton, NY 11973
2	Director Lawrence Livermore Laboratory ATTN: Dr. Ronald S. Hawke, L-156, Box 808 Dr. Jonathan K. Scudder, L-122, Box 808 Livermore, CA 94550
2	Director Los Alamos Scientific Laboratory ATTN: Dr. Clarence M. Fowler, MS970 Dr. Denis R. Peterson, MS985 Los Alamos, NM 87545

DISTRIBUTION LIST

No. of Copies	Organization
1	International Applied Physics ATTN: Dr. John P. Barber 2400 Glenheath Drive Kettering, OH 45440
1	JAYCOR ATTN: Dr. Derek Tidman 205 S. Whiting Street Alexandria, VA 22304
2	R&D Associates ATTN: Mr. Ronald Cunningham Dr. Peter Turchi P.O. Box 9695 4640 Admiralty Way Marina Del Rey, CA 90291
2	Science Applications, Inc. ATTN: Dr. Jad H. Batteh Mr. S. Howie 6600 Powers Ferry Road Suite 220 Atlanta, GA 30339
1	Systems Planning Corporation ATTN: Mr. Andrus Villu 1500 Wilson Boulevard Arlington, VA 22209
1	Westinghouse Research and Development Laboratory ATTN: Dr. Ian R. McNab 1310 Beulah Road Pittsburgh, PA 15253
2	Massachusetts Institute of Technology Francis Bitter National Magnet Laboratory ATTN: Dr. Henry H. Kolm, Mr. Peter Mongau NW-14-3102 170 Albany Street Cambridge, MA 02139
2	University of Florida Department of Engineering Sciences ATTN: Professor K.T. Millsaps Professor B.M. Leadon Gainesville, FL 32603
1	University of Tennessee Space Institute ATTN: Professor D.R. Keefer Tullahoma, TN 37388
2	University of Texas Center for Electromechanics ATTN: Dr. Richard A. Marshall Mr. William F. Weldon 167 Taylor Hall Austin, TX 78712

Aberdeen Proving Ground

Dir, USAMSAA
ATTN: DRXSY-D
DRXSY-MP, H. Cohen
Cdr, USATECOM
ATTN: DRSTE-TO-F
Dir, USACSL, Bldg. E3516
ATTN: DRDAR-CLB-PA

USER EVALUATION OF REPORT

Please take a few minutes to answer the questions below; tear out this sheet and return it to Director, US Army Ballistic Research Laboratory, ARRADCOM, ATTN: DRDAR-TSB, Aberdeen Proving Ground, Maryland 21005. Your comments will provide us with information for improving future reports.

1. BRL Report Number _____

2. Does this report satisfy a need? (Comment on purpose, related project, or other area of interest for which report will be used.)

_____

_____

_____

3. How, specifically, is the report being used? (Information source, design data or procedure, management procedure, source of ideas, etc.) _____

_____

_____

4. Has the information in this report led to any quantitative savings as far as man-hours/contract dollars saved, operating costs avoided, efficiencies achieved, etc.? If so, please elaborate.

_____

_____

5. General Comments (Indicate what you think should be changed to make this report and future reports of this type more responsive to your needs, more usable, improve readability, etc.) _____

_____

_____

_____

6. If you would like to be contacted by the personnel who prepared this report to raise specific questions or discuss the topic, please fill in the following information.

Name: _____

Telephone Number: _____

Organization Address: _____

_____

_____